ORIGINAL PAPER

Domain-specific function of ShcC docking protein in neuroblastoma cells

Izumi Miyake[1,2], Yuko Hakomori[1], Yoko Misu[2], Hisaya Nakadate[2], Nobuo Matsuura[2], Michiie Sakamoto[3] and Ryuichi Sakai*[1]

[1]Growth Factor Division, National Cancer Center Research Institute, 5-1-1 Tsukiji, Chuo-ku, Tokyo 104-0045, Japan; [2]Department of Pediatrics, Kitasato University School of Medicine, 1-15-1 Kitasato, Sagamihara-shi, Kanagawa 228-8555, Japan; [3]Department of Pathology, Keio University School of Medicine, 35 Shinanomachi, Shinjuku-ku, Tokyo 160-8582, Japan

ShcC is a family member of the Shc docking proteins that possess two different phosphotyrosine-binding motifs and conduct signals as Grb2-binding substrates of various receptor tyrosine kinases. We have recently shown that some neuroblastoma cell lines, such as NB-39-nu cells, express a protein complex of hyperphosphorylated ShcC and anaplastic lymphoma kinase (ALK), which is self-activated by gene amplification. Here, we demonstrate that the expression of a mutant ShcC lacking Grb2-binding sites, 3YF-ShcC, significantly impaired the survival, differentiation and motility of NB-39-nu cells by blocking the ERK and Akt pathways. On the other hand, cells overexpressing ShcC or 3YF-ShcC, but not a mutant ShcC that lacks SH2, showed decreased anchorage independency and in vivo tumorigenicity, suggesting a novel ShcC-specific suppressive effect through its SH2 domain on cell transformation. Notably, overexpression of ShcC suppressed the sustained phosphorylation of Src family kinase after cell detachment, which might be independent of phosphorylation of Grb2-binding site. It was indicated that the Src/Fyn-Cas pathway is modulated as a target of these suppressive effects by ShcC. Reciprocal change of ShcC expression and phosphorylation observed in malignant neuroblastoma cell lines might be explained by these phosphotyrosine-dependent and -independent functions of ShcC.
Oncogene (2005) 0, 000–000. doi:10.1038/sj.onc.1208523

Keywords: ShcC; neuroblastoma; dominant-negative form; SH2 domain; Src family kinase

Introduction

The Shc family of docking proteins plays an essential role in leading cellular signaling to specific downstream molecules such as the Ras-ERK pathway and the phosphatidylinositol 3-kinase (PI3 K)-Akt pathway when recruited towards phosphotyrosine residues of various activated RTKs. In mammals, three *shc* genes

have been identified, and their products have been termed ShcA/Shc, ShcB/Sli/Sck and ShcC/Rai/N-Shc (Nakamura et al., 1996a; O'Bryan et al., 1996b; Pelicci et al., 1996). ShcA is ubiquitously expressed in most organs except the adult neural system, whereas ShcB and ShcC proteins are selectively expressed in the neural system within adult mouse tissues.

The Shc family molecules have a unique PTB-CH1-SH2 modular organization. Two phosphotyrosine-binding modules, PTB and SH2 domains, recognize phosphotyrosine-containing polypeptides such as cytoplasmic domains of various activated RTKs (Pelicci et al., 1992; van der Geer et al., 1995). The CH1 domain has several tyrosine phosphorylation sites that recruit other SH2-containing adaptor molecules such as Grb2 (van der Geer et al., 1996; Thomas and Bradshaw, 1997) and a proline-rich stretch of ShcA composing the binding site for the SH3 domains of other proteins including Src, Fyn and Lyn (Weng et al., 1994; Wary et al., 1998). There might be difference in the molecular functions of each Shc family member, although there is not much information on individual roles of Shc families in the neural system and neuronal tumors.

We have recently shown that the expression and tyrosine phosphorylation of Shc family proteins, especially ShcC, are observed in most neuroblastoma cells. Stable association of constitutively activated anaplastic lymphoma kinase (ALK) with the ShcC has been observed in several neuroblastoma cell lines that have extremely high phosphorylation levels of ShcC (Miyake et al., 2002). These cell lines showed malignant phenotypes as for tumorigenicity in nude mice or soft agar colony assay, and notably, ShcC expression is low compared with other neuroblastoma in spite of significantly high phosphorylation state. The *ALK* gene locus was significantly amplified in these cell lines, which results in the constitutive activation of the ALK and most prominent tyrosine phosphorylation of ShcC among several known binding partners of ALK such as PLCγ and IRS-1 (Miyake et al., 2002).

ALK protein has the typical structure of an RTK classified into the insulin receptor superfamily. It is dominantly expressed in the normal neural system (Iwahara et al., 1997; Morris et al., 1997), although the biological role of this protein in neuronal cells has not yet been clearly identified. We detected remarkable

Gml : Ver 6.0 Template: Ver 6.1	Journal: ONC	☐ Disk used	Despatch Date: 4/2/2005

Article : npg_onc_2004-01698
Pages: 1-10   OP: vimala

IV - 306

amplification of the *ALK* gene in three out of 13 neuroblastoma cell lines (Miyake et al., 2002) and a less significant gain of copy numbers in eight out of 85 primary neuroblastoma tissues (Hakomori et al., manuscript in preparation), most of which accompany the amplification of the *N-myc* gene. The three *ALK*-amplified neuroblastoma cell lines showed constitutive activation of full-length ALK and the increased local concentration of receptor tyrosine kinases appeared to interfere with signals from other RTKs. It is possible that ALK-ShcC signal activation has additional effects on the malignant tumor progression of neuroblastoma, probably similar to the mechanism reported in EGFR and Neu/ErbB2 (Andrechek et al., 2000; Pawson et al., 2001).

To clarify the role of hyperphosphorylated ShcC in neuroblastoma cells, the 3YF-ShcC mutant, which has phenylalanines at three Grb2-binding tyrosines (Y221/222/304) of ShcC, was utilized in this study in the expectation of a dominant-negative effect specific for signals originating from the ShcC-Grb2 complex. The biological effects of the 3YF-ShcC mutant as well as wild-type ShcC and the ΔSH2 ShcC mutant, which lacks the SH2 domain, were analysed to elucidate both Grb2-dependent and -independent functions of ShcC in neuroblastoma.

Results

Suppression of ERK1/2 and Akt activation in NB-39-nu cells by expression of 3YF-ShcC

A neuroblastoma cell line, NB-39-nu, was used in this study because it shows high tumorigenicity and anchorage independency with prominent phosphorylation level of ShcC caused by constitutively activated ALK kinase. The expression level of ShcC is relatively low among the neuroblastoma cell lines examined in our previous study. T7-tagged ShcC constructs containing the full length of human ShcC cDNA (ShcC-wt), a tyrosine-to-phenylalanin mutant for all three putative Grb2-binding sites (3YF-ShcC), and the SH2-deletion mutant (ΔSH2-ShcC) were subcloned into a mammalian expression vector, pcDNA3.1. Multiple independent clones of NB-39-nu cell lines stably expressing these ShcC mutants at comparable levels were selected and submitted to biochemical and biological analysis. Results of representative clones are shown in Figure 1a, although basically same results were obtained from other independent clones (data not shown). Tyrosine phosphorylation of the 3YF-ShcC was significantly suppressed suggesting that the three tyrosines lost in this mutant are the main phosphorylation sites of ShcC in NB-39-nu (Figure 1a). As expected, the complex formation of 3YF-ShcC with Grb2 was impaired, regardless of EGF stimulation, compared with that of ShcC-wt and ΔSH2-ShcC (Figure 1c). The activation level of ERK1/2 at 5 min after the EGF stimulation was decreased by expression of 3YF-ShcC, while expression of ShcC-wt or ΔSH2-ShcC did not affect the levels of

ERK1/2 activation compared with the control cells transfected only by expression vector (mock) (Figure 1d). The phosphorylation level of Akt at Ser-473 was also suppressed by expression of 3YF-ShcC, although not at a similar level as that of cells treated with Wortmannin (Sigma), a PI3K inhibitor (Figure 1e). These analyses were performed using at least two independent clones. It was confirmed that 3YF-ShcC-expression has a dominant-negative effect on the PI3K/Akt pathway as well as the Ras/ERK pathway in this neuroblastoma cell line.

Expression of 3YF-ShcC increased susceptibility to retinoic acid (RA)-induced apoptosis in NB-39-nu cells

There were no obvious differences in growth rate among the NB-39-nu clones expressing each ShcC mutant (Figure 2a), whereas the rate of [^{3}H]-thymidine incorporation of the cell lines expressing 3YF-ShcC was slightly lower than that of other cells (Figure 2b).

The cytological analyses of the cells cultured with 10 μM of all-*trans*-RA revealed that 3YF-ShcC expressing cells were more susceptible to RA-induced apoptosis than the control or ShcC-wt-expressing cells (Figure 3a). Treatment of NB-39-nu cells, especially ShcC-wt-expressing cells, with RA at a lower concentration of 2.5 or 5 μM induced mild neurite formation, flattened, substrate-adherent cells resembling epithelial cells within 48 h (Figure 3b), which is known to be a characteristics of RA-induced morphologic differentiation (Sidell et al., 1983). In contrast, this type of differentiation was not observed in 3YF-ShcC-expressing cells. Along with the suppressive effects of 3YF-ShcC to the Akt pathway (Figure 1e), these results suggest that phosphorylated ShcC plays significant role in survival signals through the putative Grb2-binding sites in NB-39-nu cells.

ShcC plays a distinct role in the migration of ALK-ShcC-activated neuroblastoma cells

Expression of 3YF-ShcC significantly suppresses cell migration ability as shown by the wound-healing assay (Figure 4a). A modified Boyden chamber cell-migration assay without Matrigel using fibronectin as a chemoattractant showed the results consistent with those obtained in the wound-healing assay (Figure 4b). A similar assay with Matrigel coating on a chamber filter to evaluate the chemotactic invasive activity of each transfectant also showed decreased invasive activity in 3YF-ShcC-expressing cells (Figure 4c). In contrast, ShcC-wt expression increased the migration ability of NB-39-nu cells both in wound healing assay and modified Boyden chamber assay without Matrigel (Figure 4a, b), while the ΔSH2-ShcC expression presented no remarkable effects on the cell motility. The invasive activity of ShcC-wt-expressing cells was not significantly high compared to that of the control or of the ΔSH2-ShcC-expressing cells (Figure 4c).
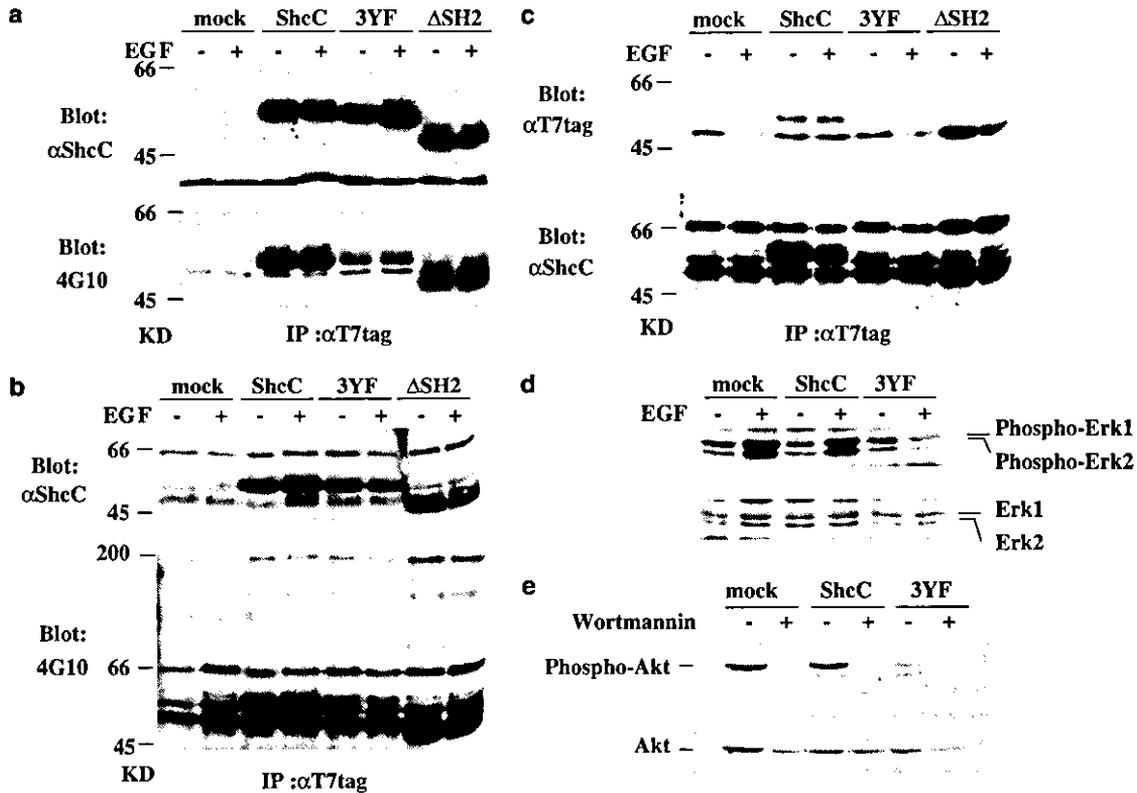
Figure 1 NB-39-nu cells stably expressing ShcC mutants analysed by immunoblotting. (a) Expression (upper panel) and tyrosine phosphorylation (lower panel) of ectopic ShcC mutant proteins (mock: control, ShcC: ShcC-wt, 3YF: 3YF-ShcC and ΔSH2: ΔSH2-ShcC) in the NB-39-nu cells. (b) Expression (upper panel) and tyrosine phosphorylation (lower panel) of both endogenous ShcC and ectopic ShcC mutants in NB-39-nu cells. (c) The complex formation of Grb2 with ShcC (lower panel) or ectopic ShcC mutants (upper panel) was analysed. (d) The activation of ERK1/2 in ShcC mutant cells. (e) Akt (Ser473) phosphorylation in ShcC mutant cells in a tissue culture medium with 10% fetal calf serum (FCS). For the negative control, the cells were treated with 1 μM of Wortmannin for 2 h. EGF stimulations were performed as described in Materials and methods. Lysates were duplicated and detected by the antibodies shown in the figure

Expression of ShcC-wt or 3YF-ShcC has a negative effect on the transforming activity of NB-39-nu cells

Cells expressing ShcC-wt or 3YF-ShcC tend to grow to confluence with a monolayer appearance, making a clear difference from original NB-39-nu cells that tend to form cell aggregations on the culture dishes (Figure 5a). In addition, control NB-39-nu cells and ΔSH2-ShcC-expressing cells form a considerable number of colonies in soft agar (Figure 5b), which is significantly suppressed by the expression of ShcC-wt or 3YF-ShcC (Figure 5b). These results indicate that ShcC-wt or 3YF-ShcC have inhibitory effect on the transforming activity of NB-39-nu cells, especially anchorage-independent growth. Since the overexpression of ShcC had no significant effect on the activation of ERK1/2 or Akt in our experiment, it was suggested that a unique signaling pathway rather than classical Grb2-Ras pathway is involved in this phenomenon.

Src family kinases (SFKs) are well known to be associated with the ability to induce cellular transformation including anchorage independency (Parsons and Weber, 1989; Windham et al., 2002). During the

investigation of ShcC mutant cells in the suspension state, we noticed that the sustained activation of both Fyn and c-Src observed in the control cells and ΔSH2-ShcC-expressing cells was suppressed by the expression of ShcC-wt or 3YF-ShcC (Figure 6a, b) at 24 h after cell detachment. Especially, the condition of phosphorylation of Fyn at suspension culture well correlated with anchorage independency of NB-39-nu sublines (Figure 6a). Tendency of phosphorylation of Src Tyr-416, which indicates the kinase activation of SFKs, is consistent with these results (Figure 6c). Phosphorylation of Cas, a main substrate of SFKs, in a suspended condition has recently been associated with the anchorage-independent growth of cancer-like lung adenocarcinoma (Wei et al., 2002). Sustention and temporary elevation of the Cas phosphorylation was also observed specifically in the original NB-39-nu cells, control and ΔSH2-ShcC-expressing cells, whereas there was a marked decrease of the phosphorylation level of Cas in ShcC-wt- and 3YF-ShcC-expressing cells (Figure 6d, e). Treatment of NB-39-nu control cells with PP2, a Src-specific inhibiter, suppressed the phosphorylation of Cas both in an attached and suspended condition, suggesting
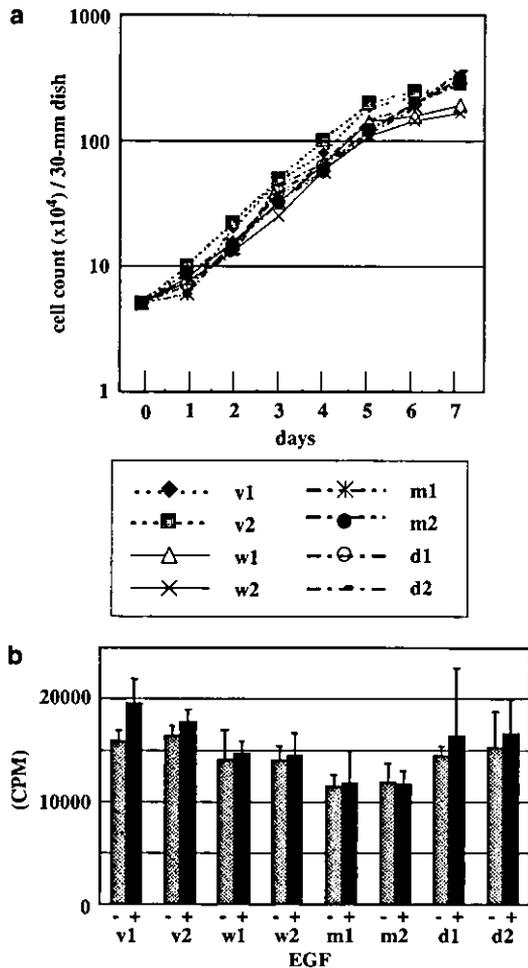
Figure 2 Growth rate and proliferation ability of ShcC mutant cells *in vitro*. (a) ShcC mutant cells cultured in a normal medium with 10% FCS by 30-mm dishes were counted at the indicated time points. The results represent the average values (±s.d.) of three replicated experiments for each clone. (b) ShcC mutant cells stimulated with none (gray bar) or EGF (black bar) were treated with [³H]thymidine to the culture medium as described in Materials and methods. The graph represents the average values (±s.d.) from an experiment performed in triplicate. NB-39-nu clones are described as: v1 and v2 (control), w1 and w2 (expressing ShcC-wt), m1 and m2 (expressing 3YF), d1 and d2 (expressing ΔSH2)

that the anchorage-independent phosphorylation of Cas is associated with the activity of the SFKs (Figure 6f).

The activation of ERK1/2 or Akt was similarly suppressed by suspension culture for 24 h regardless of the expression of each ShcC mutants although the basal level is lower in 3YF-ShcC clones (Supplementary Figure A). There were no difference in phosphorylation level of FAK and paxillin, which plays an important role in regulating the signals from the extracellular matrix (ECM) and organizing the actin-cytoskeleton, by expressing ShcC-wt, showing a similar level of decrease in the suspended condition (Supplementary Figure B). In summary, it was confirmed in this system that the

constitutive activation of SFKs, such as Fyn and c-Src, and phosphorylation of Cas in suspended cells, but not other components of integrin signals such as FAK, is strictly linked to the anchorage independency of NB-39-nu cells, closely related with ShcC mutants expression. Furthermore, we detected interaction between ShcC-wt and some of SFKs following the stimulation (Figure 6g), indicating a novel biological interaction of ShcC with SFK, as suggested for ShcA in integrin pathway (Wary et al., 1996; Giancotti, 1997)

Loss of tumorigenicity of NB-39-nu-expressing ShcC-wt or 3YF-ShcC in mouse subcutaneous tissues

To investigate these antitransforming effects of ShcC-wt and 3YF-ShcC *in vivo*, the tumorigenicity of NB-39-nu cells expressing each mutant in nude mice was evaluated. Tumors generated by eight independent injections of each mutant were analysed in weight and histology at 4 weeks after subcutaneous injection. The results revealed a marked reduction in sizes of tumors from the cells expressing either ShcC-wt or 3YF-ShcC at this time, but not of tumors from the control cells or cells expressing ΔSH2-ShcC (Figure 7a).

The tumors from the control, ShcC-wt-expressing and ΔSH2-ShcC-expressing cells presented a hypervascular appearance (Figure 7a: upper panel), which has the histological characteristics of almost equal-sized cells with a regular arrayed pattern, high nuclear-to-cyto-plasmic (N/C) ratio and chromatin-rich nucleuses (Figure 7b). On the other hand, the tumors from the 3YF-ShcC-expressing cells were hypovascular and histologically distinct from the other mutants, showing rather unequal-sized cells with an irregular arrayed pattern, a lower N/C ratio, few mitosis and decreased nucleus density. In accordance with this, staining by a proliferation marker, Ki-67, or a mitotic activity marker, cyclin A, markedly decreased in the tumors from 3YF-ShcC-expressing cells (Figure 7b), showing that the cell cycle progression was significantly suppressed by 3YF-ShcC *in vivo*, compared with the analysis by [³H]-tymidine incorporation *in vitro* (Figure 2b). TUNEL staining showed no marked difference in cell apoptosis among each tumor tissue (data not shown). These results suggest that the antitumorigenic activity of the 3YF-ShcC-expressing cells *in vivo* accompanies the regulation of cell proliferation, which is distinct from the impairment of tumor-igenicity by expression of ShcC-wt.

Discussion

In our previous report, the biological effects of constitutively activated signals of ALK-ShcC on the tumorigenesis of neuroblastoma cells remain to be investigated. Here, we demonstrated that the proliferation, survival and cell migration of these neuroblastoma cells were dependent on the signals via ShcC-Grb2 pathway, downstream of ALK. Additionally, over-expressed ShcC has a suppressive effect on the
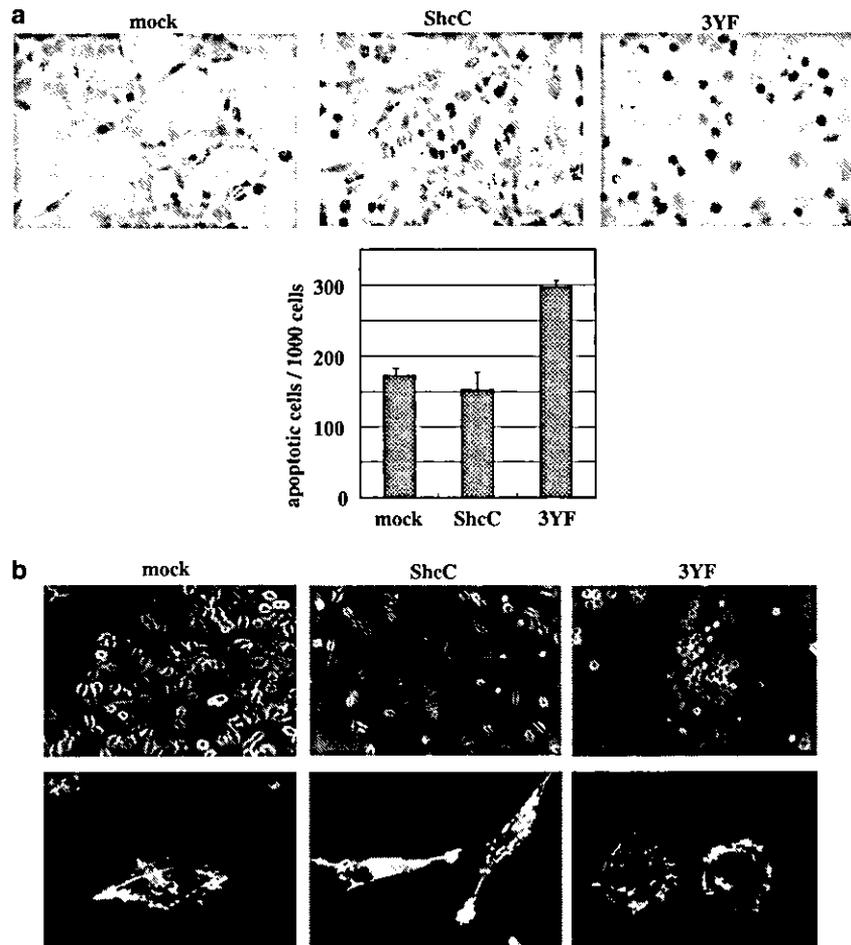
Figure 3 Effects of ShcC mutants on apoptosis and differentiation of NB-39-nu cells induced by all-*trans* retinoic acid (RA). (a) TUNEL analysis of ShcC mutant cells were performed as described in Materials and methods. Bar: 100 μm (upper panel). TUNEL-positive cells, the prominent dark positive cells, are counted for every 1000 cells for each slide, and three different slides were analysed for each sample. The graph represents the results (expressed as mean ± s.d.) of three observations (lower panel). (b) RA-induced morphological change of NB-39-nu cells expressing ShcC mutants. The cells were grown for 48 h in RPMI 1640 with 10% FCS containing 2.5 μM of RA and examined by phase-contrast microscopy (upper panel). Actin filaments stained with FITC-labeled phalloidin were visualized with a confocal fluorescence microscope (lower panel)

anchorage-independent growth of these cells via its SH2 domain and this regulation is closely associated with the regulation of c-Src and Fyn tyrosine kinases.

The fact that 3YF-ShcC significantly suppressed the activity of both ERK1/2 and Akt, suggesting that ShcC, among signaling pathways originating from activated ALK, predominantly regulates these signals through binding to Grb2. Our recent study also shows that the suppression of activated ALK using the RNA interference technique (RNAi) reduces the phosphorylation of ShcC, ERK1/2 and Akt, and induces the apoptotic cell death of NB-39-nu cells (Hakomori *et al.*, manuscript in preparation). The ERK and Akt pathways are key regulators of cell proliferation, survival and differentiation. Cells expressing 3YF-ShcC become more susceptible to RA-induced apoptosis presumably due to inhibition of the Akt pathway. It has recently

been shown that ShcC is physiologically involved in the regulation of the PI3K/Akt pathway as a downstream effecter of the ligand-stimulated Ret receptor in neuroblastoma cells (Pelicci *et al.*, 2002). This study confirms that the survival of NB-39-nu cells is regulated by the signals downstream of ShcC. The 3YF-ShcC also causes inhibition of cell motility, while overexpressed ShcC significantly increases the ability of cell migration, indicating that ShcC positively affects the regulation of cell migration. Previously, ShcA was shown to be closely related with cell motility via the MAPK pathway (Collins *et al.*, 1999; Gu *et al.*, 1999), but the association of ShcC with the ability of cell migration has not been investigated.

The expression of 3YF-ShcC had a suppressive effect on the proliferation of NB-39-nu cells cultured *in vitro* and more significantly on the cell cycle progression of
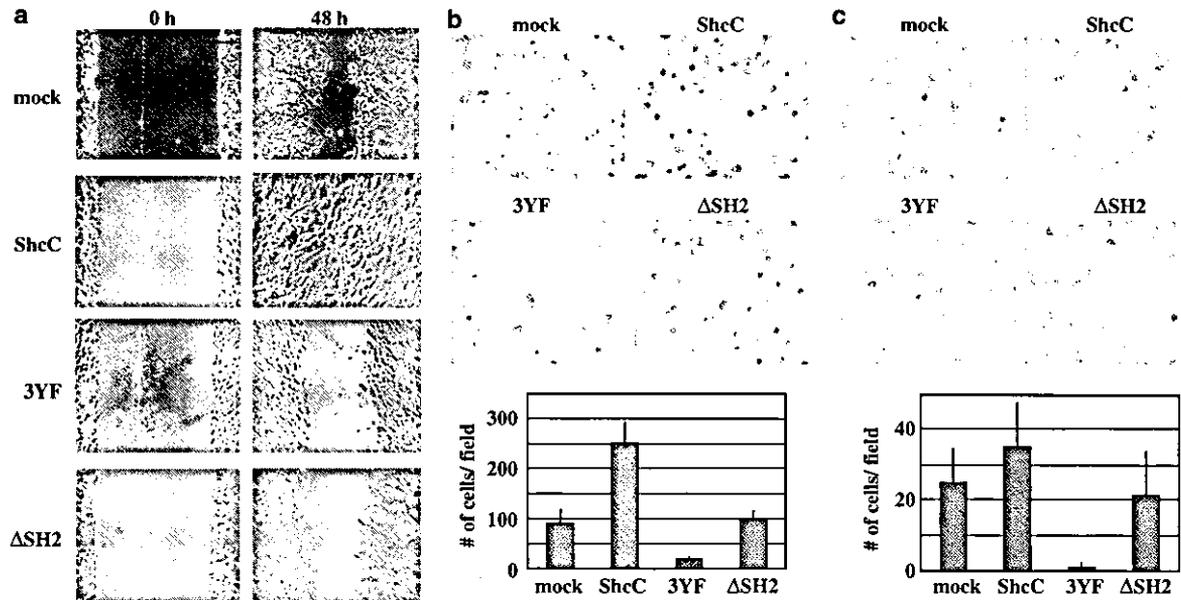
6

Figure 4 Expression of ShcC-wt significantly promotes the ability of cell migration in NB-39-nu cells. (a) Wound-healing assay for ShcC mutant cells. Photographs of the cells taken 48 h after wounding under a microscope. Bar: 200 μm. (b) Photographs (upper panel) and graph (lower panel) of ShcC mutant cells that have migrated through the filter by modified Boyden chamber cell migration assay. The graph represents the results (expressed as mean±s.d.) of the experiments performed in triplicate. (c) Photographs (upper panel) and a graph (lower panel) of the results from cell invasion assay
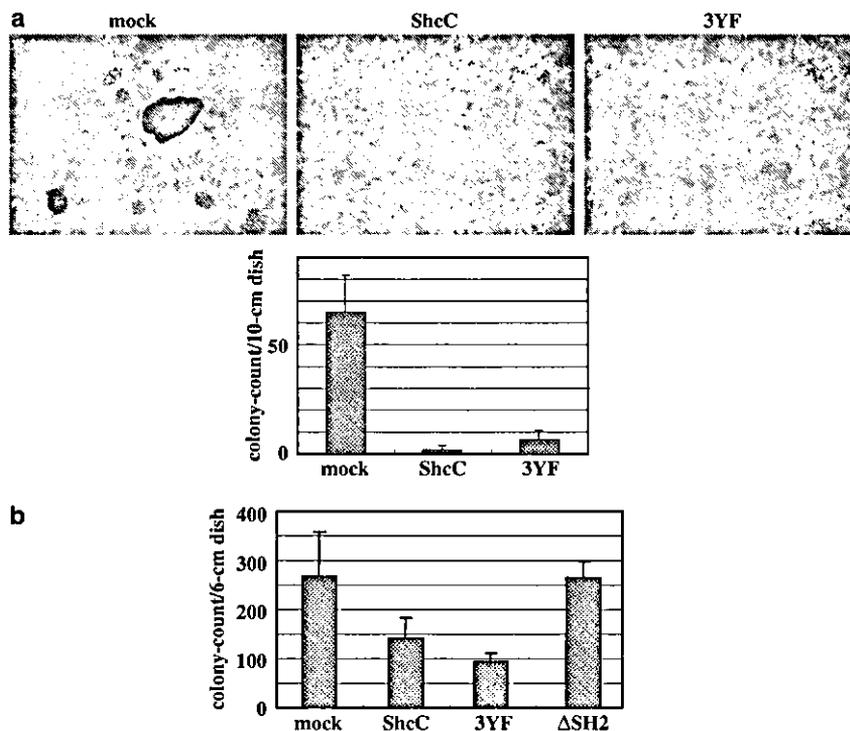

Figure 5 Evaluation of in vitro transforming activity in NB-39-nu cells expressing ShcC mutants. (a) Tendency for ShcC mutant cells to form cell aggregations on the dish surface as described in Materials and methods. Photographs of each dish were taken with a microscope at a magnification of × 40 (upper panel). The graph represents the mean values (±s.d.) of three independent experiments (lower panel). (b) Anchorage-independent growth of ShcC mutant cells was evaluated by assaying colony formation in soft agar (performed as described in Materials and methods). The results represent the average values (±s.d.) of three replicated experiments
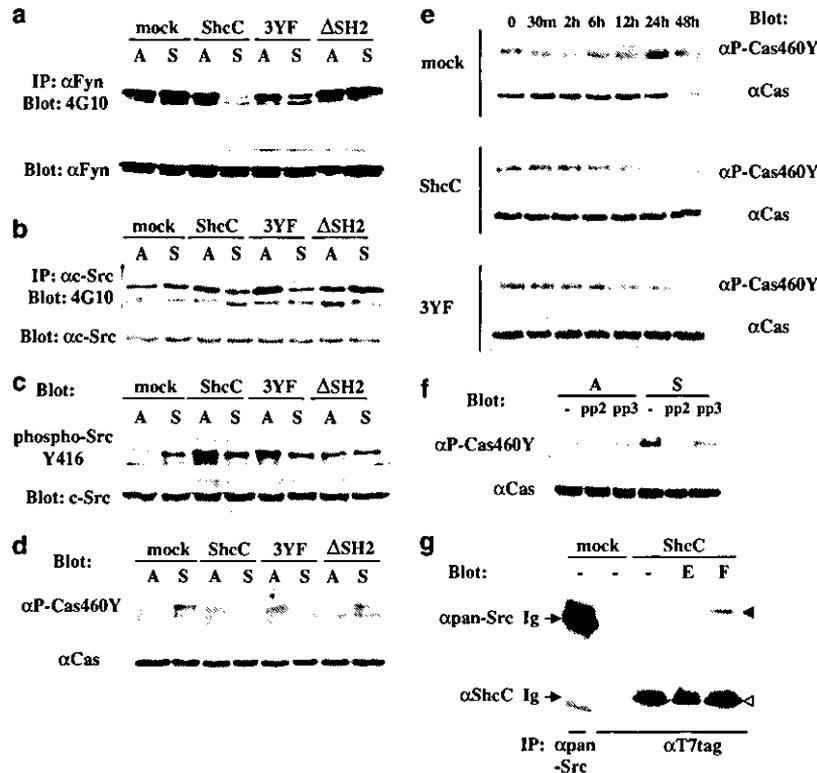
Figure 6 Anchorage-independent activation of Src family kinases (SFKs) and tyrosine phosphorylation of Cas in NB-39-nu is affected by the expression of ShcC. The cell suspension culture of ShcC mutant cells was essentially performed as described in Materials and methods. A: attached cells. S: cells in a suspended condition. Lysates were duplicated and detected by immunoprecipitation and Western analysis. (a, b and c) Cells cultured for 24 h in adherent or suspended conditions were analysed with the antibodies against each Src family kinase shown in the figure. Anti-phospho-Src Y416 recognizes all Src family members phosphorylated at the tyrosine corresponding to Tyr416 of avian Src. (d) Same analysis performed as (a) (b) and (c) using the antibodies against for phospho-460Y of Cas (αP-Cas460Y) and Cas protein (αCas). (e) Time course of tyrosine phosphorylation of Cas in each ShcC mutant cells cultured in suspension for the indicated time periods. (f) Effect of Src inhibitor, PP2, on the tyrosine phosphorylation of Cas in NB-39-nu control cells. The cells cultured for 24 h were harvested following treatment with 10 μM of PP2 for 2 h. As a negative control, the same dose of PP3 was used in place of PP2. (g) ShcC forms complex with SFKs following the stimulation of fibronectin. Lysates of mock cells and ShcC-wt cells were analysed after the stimulation with EGF or fibronectin as described in Materials and methods. -: serum free without stimulation; E: stimulated by EGF; F: stimulated by fibronectin. Ig: immunoglobulin. Anti-pan-Src antibody (SRC2) reacts with c-Src p60, Yes p62, Fyn p59, c-Fgr p55 and c-Src2. closed arrowhead: SFK; open arrowhead: p52 ShcC

the nude mouse tumor. These data suggest that ShcC positively regulates the cell proliferation of neuronal tumor cells as well as ShcA, which has been reported to affect the tumor growth in nude mice using breast cancer cell lines (Stevenson et al., 1999).

The overexpression of ShcC-wt endowed NB-39-nu cells with several characteristics. Other than the enhancement of cell migration and neurite outgrowth, which is consistent with previous study (Collins et al., 1999; Pelicci et al., 2002), the observation that ShcC-wt-expressing cells were impaired for anchorage-independent growth and tumorigenicity suggests a novel function of ShcC. Taking into account that the expression of 3YF-ShcC but not ΔSH2-ShcC showed similar effects, the SH2 domain of ShcC may be responsible for this unique function of ShcC, distinct from ShcA. In addition, the least changes in ERK1/2 or Akt activation by overexpression of ShcC-wt suggest

that this function might be independent of phosphorylation of Grb2-binding sites or the activation levels of downstream targets. There are reports showing different binding specificity towards phosphotyrosine-containing motifs among Shc families (O'Bryan et al., 1996a, b; Pelicci et al., 1996). It is crucial to identify the molecules associating with the SH2 domain of ShcC in neuroblastoma cells to elucidate the mechanism of these SH2-mediated effects of ShcC.

The smaller size of the nude mouse tumors due to the expression of ShcC-wt, regardless of mild changes in cell proliferation as both tumor tissue and culture cells, may also reflect suppression of anchorage independency (Freedman and Shin, 1974; Kumar, 1998), which results in the loss of the majority of the injected cells by anoikis before they start forming tumors. The anchorage independency of NB-39-nu mutants well corresponded to the sustained phosphorylation levels of c-Src, Fyn
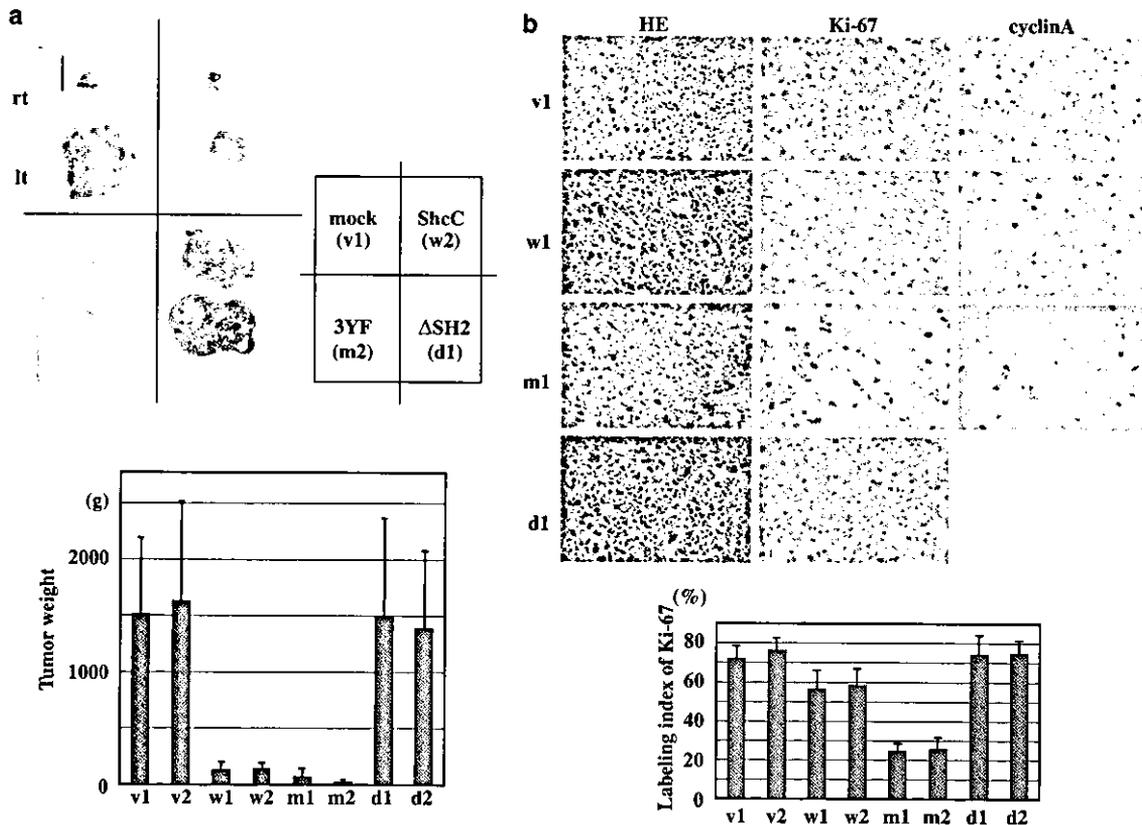
Figure 7 Nude mouse tumors derived from ShcC mutant cells. (a) Photographs of tumors from nude mice at three weeks after subcutaneous injection of ShcC mutant cells (upper panel). Tumorigenicity shown by the average weight (±s.d.) of the eight tumors derived from each clone (lower panel). Two independent clones are analysed for each ShcC mutant. Bar: 10 mm (b) Photographs of a cross-section of each tumor tissue using a microscope at a magnification of ×400. HE: tumor tissues stained with hematoxylin and eosin; Ki-67 and cyclin-A: tumor tissues immunostained against Ki-67 and cyclin-A, respectively (upper panels). The proliferating activity of each tumor was defined as the labeling index of Ki-67 by counting the positive stained cells per 1000 tumor cells. The data show the average scores±s.d. of the positive cells in three different areas of each slide (lower panel). NB-39-nu clones are described as: v1 and v2 (control), w1 and w2 (expressing ShcC-wt), m1 and m2 (expressing 3YF-ShcC), d1 and d2 (expressing ΔSH2-ShcC)

and Cas after cell detachment, suggesting that the expression of ShcC-wt has a negative effect on anchorage independency due to the suppression of the SFK-Cas pathway (Figure 6). It is possible that ShcC-SH2 plays a competitive role with YDYV in the Src-binding domain of Cas, judging from the consensus motifs binding to ShcC-SH2 (O'Bryan et al., 1996a, b), although this association was not detected by usual immunoprecipitation experiments (data not shown). On the other hand, the fact that ShcC forms the complex with SFK in this study indicates that there might be a role of association between SFK and ShcC in the regulation of tyrosine kinase activity of SFK. The fact that malignant neuroblastoma cell lines with hyperphosphorylated ShcC frequently have lower expression level of ShcC (Miyake et al., 2002) might indicate additive effects of hyperphosphorylation and downregulation of ShcC on phenotype of neuroblastoma. There is the possibility that an unknown mechanism causes down-regulation of ShcC, which is hyperphosphorylated by

receptor stimulation, and eventually induces malignant transition of tumors.

We have shown in this study that hyperphosphory-lated ShcC in neuroblastoma cells plays an essential role in regulating cellular proliferation, survival, migration and transformation, and each domain of ShcC might differentially regulate these physiological functions. Controlling these domain-mediated signals could be a target in restricting the progression and metastasis of neuroblastoma cells.

Materials and methods

Plasmid constructions

Tyrosine-to-phenylalanine mutations were introduced in the ShcC cDNAs by in vitro site-directed mutagenesis, which changed Y221/222 and Y304 to three phenylalanines (3YF-ShcC). The SH2 domain (amino acid 379–472)-deleted form of

ShcC (ΔSH2-ShcC) was also generated. All parts amplified by PCR were verified by sequencing.

Cell culture, transfection

NB-39-nu cells were used in our previous report (Miyake et al., 2002). The stable expression of ShcC mutants, the full-length of ShcC (ShcC-wt), 3YF-ShcC and ΔSH2-ShcC in NB-39-nu cells were obtained by transfection using Fugene™ 6 transfection reagent (Roche Molecular Biochemicals) according to the manufacturer's instructions. Then, cell clones were obtained from individual G418-resistent colonies and subjected to Western blot screening using the T7 tag antibody (Novagen). These cells were cultured in an RPMI 1640 medium with 10% FCS (Sigma) at 37°C in 5% CO_2. A suspension culture of the cells was essentially performed according to a previously published procedure (Folkman and Moscona, 1978; Frisch and Francis, 1994; Wang and Sheibani, 2002). In this study, LOW-CELL-BINDING 90 mm-Petri dishes treated with 2-Methacryloxyethyl Phosphorylcholine (MPC) (Nalge Nunc International) were used instead of poly-HEMA-coated dishes. The cells were grown to confluence in tissue culture dishes, and were then trypsinized and plated at a concentration of 1 × 10⁶ cells/90 mm dish into MPC-treated Petri dishes and cultured for 0–48 h. The cells were then collected by pipetting, washed by PBS and extracted with PLC-lysis buffer (Rozakis-Adcock et al., 1993) for the Western analysis.

Preparation of specific antibodies, cell stimulation, immunoprecipitation and immunoblotting

The polyclonal antibodies against the CH1 domains of ShcC (amino acid 306–371) and against Cas protein (αCas) were prepared as described (Sakai et al., 1994, 2000). A phospho specific polyclonal antibody against Cas (αP-Cas460Y) was generated by immunizing rabbits with a synthetic peptide, CAEDV(pY)DVP, which is a representative of the repetitive tyrosine-containing motifs in the substrate domain of Cas, after being conjugated with thyroglobulin. Other antibodies were purchased as follows: anti-phosphotyrosine antibody (4G10) (Upstate Biotechnology, Inc), anti-p44/42 MAPK (ERK1/2) and anti-phospho-p44/42 MAPK (phospho-ERK1/2) antibodies (BioLabs), anti-Akt and anti-phospho-Akt (Ser473) antibodies (Cell Signaling), anti-c-Src antibody (Upstate Biotechnology, Inc.), anti-phospho Src family (Tyr416) antibody (Cell Signaling), anti-Fyn antibody and anti-pan-Src antibody (SRC2) (SantaCruz Biotechnology, Inc.). As secondary antibodies, horseradish peroxidase (HRP)-conjugated anti-rabbit and anti-mouse Ig (Amersham) were used. Cell-stimulation analysis with epidermal growth factor (EGF; Wako) was performed as described. The cells were starved for 24 h and treated for 5 min with EGF (100 ng/ml) (Miyake et al., 2002). As for stimulation with fibronectin, cultured cells were starved for 24 h then trypsinized without FCS and after the suspending condition for 30 min, seeded onto fibronectin (10 μg/ml)-coated dishes and harvested after 1 h using PLC lysis buffer. Control cells were harvested before the attachment on the fibronectin-coated surface. The immunoprecipitation and Western analysis were performed using the procedure described in the previous report (Miyake et al., 2002).

Evaluation of tendency to form cell aggregations on dish surface

Cells were seeded onto plastic dishes (1 × 10⁶ cells per 100-mm diameter dish). After 5 days, distinctive colonies of cell aggregations proliferated independently of the attachment to the dish surface, and each of them consisted of more than 10

cells per dish. The data were obtained from three independent experiments.

Soft agar colony-formation assay

Anchorage-independent growth was determined by assaying colony formation in soft agar as described in the previous report (Honda et al., 1998). Briefly, 10⁵ trypsinized cells were resuspended in DMEM containing 10% FCS and 0.4% Sea Plaque GTG agarose (Bioproduct) and poured onto bottom agar containing 10% FCS and 0.53% agarose in 6-cm culture dishes. The cells were then incubated at 37°C with 5% CO_2. After 14 days, colonies containing more than five cells were counted under the microscope.

Wound-healing assay

A wound-healing assay was performed according to the method used previously (Honda et al., 1999). Briefly, cells were grown to confluence in Matrigel-coated plastic culture dishes, and a wound was made using a sterile micropipette tip. Cell movement was assessed 24 and 48 h after wounding under the microscope at a magnification of × 100.

Cell migration and invasion assay

Cell invasion was analysed according to the procedure of the Boyden chamber cell migration assay with some modification (Honda et al., 1999), using a FALCON™ Cell Culture Insert, a chamber with a pore size of 8 μm (Becton Dickinson Labware) whose interior was filled with a plug of 10 μg Matrigel (IWAKI) per filter. A total of 1 × 10⁵ cells in 200 μl of serum-free medium were plated in the Matrigel chamber, and a serum-free medium containing 50 μg/ml of fibronectin was placed in the 24-well plate as a lower chamber, then incubated for 12 h at 37°C in 5% CO_2. The number of cells migrated through the Matrigel to the underside of the filter was counted under the microscope. The same procedure was performed without Matrigel coating for the analysis of cell migration.

Apoptosis of neuroblastoma cells induced by all-trans RA

Cells, were seeded into 24-well tissue culture plates at a density of 5 × 10⁴ cm⁻² and cultured in the presence of the indicated concentration of RA (all-trans form; Sigma) dissolved in 70% ethanol. Control cultures were treated with the same concentration of ethanol. To identify RA-induced apoptotic reaction, TUNEL (TdT-mediated dUTP-biotin nick end labeling) was performed according to the manufacturer's instructions (In Situ Cell Death Detection, POD: Roche) as described by Gavrieli et al. (1992). The cells were counterstained with hematoxylin-eosin.

[³H]thymidyne incorporation assay

This was performed essentially as described previously (McNeil et al., 1985). A total of 2 × 10⁴ cells were seeded onto 24-well dishes and cultured for 48 h and shifted to a serum-free medium, and then 24 h later were followed by overnight stimulation with 100 ng/ml EGF. [³H]thymidine (1 μCi/ml) was added for the last 4 h of incubation. The amount of incorporated [³H]thymidine radioactivity was measured by liquid scintillation counting. Results are expressed as disintegrations per minute of incorporated [³H]thymidine per well.

Generation of tissue samples and histological evaluation

Nude mouse tumors were obtained by independent injections of 5×10^6 ShcC mutant cells into the bilateral subcutaneous tissues of each mouse. Tumor tissues were fixed in formalin at 4°C, transferred to 70% ethanol, and blocked in paraffin. Sections were stained with hematoxylin and eosin.

Immunohistochemistry

The sections of the tumor tissues from ShcC mutant cells were immunostained with anti-Ki-67 antibody (DAKO) and anti-cyclin-A antibody (Novocastra Laboratories) using the labeled

streptavidin biotin (LSAB) methods according to the manufacturer's instructions of the LSAB kit (Dako). All the primary antigens were used at a 1:100 dilution. Peroxidase activity was visualized with 3, 3'-diaminobebenzidine (DAB).

References

Andrechek ER, Hardy WR, Siegel PM, Rudnicki MA, Cardiff RD and Muller WJ. (2000). *Proc. Natl. Acad. Sci. USA*, **97**, 3444–3449.
Collins LR, Ricketts WA, Yeh L and Cheresh D. (1999). *J. Cell Biol.*, **147**, 1561–1568.
Folkman J and Moscona A. (1978). *Nature*, **273**, 345–349.
Freedman VH and Shin SI. (1974). *Cell*, **3**, 355–359.
Frisch SM and Francis H. (1994). *J. Cell Biol.*, **124**, 619–626.
Gavrieli Y, Sherman Y and Ben-Sasson SA. (1992). *J. Cell Biol.*, **119**, 493–501.
Giancotti FG. (1997). *Curr. Opin. Cell. Biol.*, **9**, 691–700.
Gu J, Tamura M, Pankov R, Danen EH, Takino T, Matsumoto K and Yamada KM. (1999). *J. Cell Biol.*, **146**, 389–403.
Honda H, Nakamoto T, Sakai R and Hirai H. (1999). *Biochem. Biophys. Res. Commun.*, **262**, 25–30.
Honda H, Oda H, Nakamoto T, Honda Z, Sakai R, Suzuki T, Saito T, Nakamura K, Nakao K, Ishikawa T, Katsuki M, Yazaki Y and Hirai H. (1998). *Nat. Genet.*, **19**, 361–365.
Iwahara T, Fujimoto J, Wen D, Cupples R, Bucay N, Arakawa T, Mori S, Ratzkin B and Yamamoto T. (1997). *Oncogene*, **14**, 439–449.
Kumar CC. (1998). *Oncogene*, **17**, 1365–1373.
McNeil PL, McKenna MP and Taylor DL. (1985). *J. Cell Biol.*, **101**, 372–379.
Miyake I, Hakomori Y, Shinohara A, Gamou T, Saito M, Iwamatsu A and Sakai R. (2002). *Oncogene*, **21**, 5823–5834.
Morris SW, Naeve C, Mathew P, James PL, Kirstein MN, Cui X and Witte DP. (1997). *Oncogene*, **14**, 2175–2188.
Nakamura N, Chin H, Miyasaka N and Miura O. (1996a). *J. Biol. Chem.*, **271**, 19483–19488.
Nakamura T, Sanokawa R, Sasaki Y, Ayusawa D, Oishi M and Mori N. (1996b). *Oncogene*, **13**, 1111–1121.
O'Bryan JP, Martin CB, Songyang Z, Cantley LC and Der CJ. (1996a). *J. Biol. Chem.*, **271**, 11787–11791.
O'Bryan JP, Songyang Z, Cantley L, Der CJ and Pawson T. (1996b). *Proc. Natl. Acad. Sci. USA*, **93**, 2729–2734.
Parsons JT and Weber MJ. (1989). *Curr. Top. Microbiol. Immunol.*, **147**, 79–127.
Pawson T, Gish GD and Nash P. (2001). *Trends Cell Biol.*, **11**, 504–511.

Pelicci G, Dente L, De Giuseppe A, Verducci-Galletti B, Giuli S, Mele S, Vetriani C, Giorgio M, Pandolfi PP, Cesareni G and Pelicci PG. (1996). *Oncogene*, **13**, 633–641.
Pelicci G, Lanfrancone L, Grignani F, McGlade J, Cavallo F, Forni G, Nicoletti I, Pawson T and Pelicci PG. (1992). *Cell*, **70**, 93–104.
Pelicci G, Troglio F, Bodini A, Melillo RM, Pettirossi V, Coda L, De Giuseppe A, Santoro M and Pelicci PG. (2002). *Mol. Cell. Biol.*, **22**, 7351–7363.
Rozakis-Adcock M, Fernley R, Wade J, Pawson T and Bowtell D. (1993). *Nature*, **363**, 83–85.
Sakai R, Henderson JT, O'Bryan JP, Elia AJ, Saxton TM and Pawson T. (2000). *Neuron*, **28**, 819–833.
Sakai R, Iwamatsu A, Hirano N, Ogawa S, Tanaka T, Mano H, Yazaki Y and Hirai H. (1994). *EMBO J.*, **13**, 3748–3756.
Sidell N, Altman A, Haussler MR and Seeger RC. (1983). *Exp. Cell Res.*, **148**, 21–30.
Stevenson LE, Ravichandran KS and Frackelton Jr AR. (1999). *Cell Growth Differ.*, **10**, 61–71.
Thomas D and Bradshaw RA. (1997). *J. Biol. Chem.*, **272**, 22293–22299.
van der Geer P, Wiley S, Gish GD and Pawson T. (1996). *Curr. Biol.*, **6**, 1435–1444.
van der Geer P, Wiley S, Lai VK, Olivier JP, Gish GD, Stephens R, Kaplan D, Shoelson S and Pawson T. (1995). *Curr. Biol.*, **5**, 404–412.
Wang Y and Sheibani N. (2002). *J. Cell. Biochem.*, **87**, 424–438.
Wary KK, Mainiero F, Isakoff SJ, Marcantonio EE and Giancotti FG. (1996). *Cell*, **87**, 733–743.
Wary KK, Mariotti A, Zurzolo C and Giancotti FG. (1998). *Cell*, **94**, 625–634.
Wei L, Yang Y, Zhang X and Yu Q. (2002). *J. Cell. Biochem.*, **87**, 439–449.
Weng Z, Thomas SM, Rickles RJ, Taylor JA, Brauer AW, Seidel-Dugan C, Michael WM, Dreyfuss G and Brugge JS. (1994). *Mol. Cell. Biol.*, **14**, 4509–4521.
Windham TC, Parikh NU, Siwak DR, Summy JM, McConkey DJ, Kraker AJ and Gallick GE. (2002). *Oncogene*, **21**, 7797–7807.

Supplementary Information accompanies the paper on Oncogene website (http://www.nature.com/onc).

ORIGINAL PAPER

Tyrosine phosphorylation of paxillin affects the metastatic potential of human osteosarcoma

Kotaro Azuma[1,2], Masamitsu Tanaka[1], Takamasa Uekita[1], Satoshi Inoue[2], Jun Yokota[3], Yasuyoshi Ouchi[2] and Ryuichi Sakai*[1]

[1]Growth Factor Division, National Cancer Center Research Institute, 5-1-1 Tsukiji, Chuo-ku, Tokyo 104-0045, Japan; [2]Department of Geriatric Medicine, Graduate School of Medicine, The University of Tokyo, 7-3-1, Hongo, Bunkyo-ku, 113-8655, Tokyo, Japan; [3]Division of Biology, National Cancer Center Research Institute, 5-1-1 Tsukiji, Chuo-ku, Tokyo 104-0045, Japan

To acquire information on signal alteration corresponding to the changes in metastatic potential, we analysed protein tyrosine phosphorylation of low- and high-metastatic human osteosarcoma HuO9 sublines, which were recently established as the first metastatic model of human osteosarcoma. Tyrosine phosphorylation of proteins around 60, 70, and 120–130 kDa was enhanced in high-metastatic sublines. Among these proteins, the protein around 70 kDa, which was most remarkably phosphorylated, was identified as paxillin, a scaffold protein in integrin signaling. Activity of Src family kinase correlated well with metastatic potential, and a Src family kinase inhibitor, PP2, not only abolished tyrosine phosphorylation of paxillin but also impaired the motility of high-metastatic sublines. The expression of paxillin was also elevated in high-metastatic sublines, and knocking down of paxillin expression by RNAi method resulted in attenuated motility of high-metastatic cells. We also demonstrated that the phosphorylated form of paxillin is essential for the migration-promoting effect in human osteosarcoma. These findings suggest that enhanced activity of Src family kinases and overexpression of paxillin synergistically contribute to the high metastatic potential of human osteosarcoma through the hyperphosphorylation of paxillin.
Oncogene (2005) 0, 000–000. doi:10.1038/sj.onc.1208654

Keywords: osteosarcoma; pulmonary metastasis; paxillin; tyrosine phosphorylation; Src family kinase; motility

Introduction

Multiple steps of tumor metastasis are regulated by various external stimuli such as hormones, cytokines and extracellular matrices. As major mediators of these stimuli, both receptor and nonreceptor tyrosine kinases play important roles to elicit intracellular signal transduction in response to the metastatic environment of tumor cells (Pawson, 2004). Various processes such as cell adhesion, anchorage-independent growth, cell motility, and cell invasion, which are essential components of tumor metastasis, are regulated by tyrosine phosphorylation. Indeed, the activation of Src family tyrosine kinases is frequently found during proliferation and metastasis of human cancers (Yeatman, 2004), indicating that tumor progression is reflected by the activity of tyrosine kinase and phosphorylation states of substrates in metastatic tumors.

Osteosarcoma is a primary malignant bone tumor that usually affects teenagers and frequent metastasis to the lungs is a clinical characteristic of osteosarcoma. As many as 20% of patients are estimated to have pulmonary metastases at the time of diagnosis and their prognosis is extremely poor with 10–20% 5-year survival rate (Meyers et al., 1993; Tsuchiya et al., 2002). Even though patients did not have metastases at the time of diagnosis, 35–50% of them developed pulmonary metastases during treatment (Huth and Eilber, 1989; Ward et al., 1994). For this reason, pulmonary metastasis of osteosarcoma requires effective prevention and treatment.

Investigation of pulmonary metastasis of human osteosarcoma was impeded by the lack of a proper metastatic model of human osteosarcoma cell lines. Recently, Kimura et al. (2002) established human osteosarcoma cell lines with high metastatic potential to the lungs for the first time. From parental HuO9 cells, M112 and M132 were established as high-metastatic sublines, which developed more than 200 macroscopic metastatic nodules in the lungs after injection of 2×10^6 cells into the tail vein of nude mice. On the other hand, L12 and L13 are low-metastatic sublines established by the dilution plating method from the same parent HuO9 cells (Nakano et al., 2003). These sublines developed only 0–15 macroscopic nodules in the lungs after injection of 2×10^6 cells and all mice survived up to 200 days.

In order to acquire information on signal alteration corresponding to the changes in metastatic potential, we compared the profile of protein tyrosine phosphorylation by utilizing these HuO9-derived sublines. A 68 kDa cytoskeletal protein, paxillin, was identified as a

*Correspondence: R Sakai; E-mail: rsakai@gan2.res.ncc.go.jp

molecule that shows the most outstanding difference in phosphorylation state between low- and high-metastatic sublines among several phosphotyrosine-containing proteins that are differentially phosphorylated in these sublines. Paxillin has no intrinsic enzymatic activity, but it has multiple domains that interact with cytoskeletal and signaling molecules, and functions as a scaffold protein at focal adhesions (Turner, 2000; Schaller, 2001). Paxillin contains two critical tyrosine phosphorylation sites at Tyr 31 and Tyr 118 (Schaller and Parsons, 1995). These phosphotyrosines are considered to serve as docking sites for other signaling molecules, but it remains controversial whether these phosphotyrosines have promoting effect or inhibitory effect on cell motility.

In this study, we show overexpression and hyperphosphorylation of paxillin in high-metastatic sublines of human osteosarcoma, indicating that, in the case of human osteosarcoma, tyrosine phosphorylation of paxillin has a promoting effect for cell migration. We also demonstrate that elevated activity of Src family kinases in high-metastatic sublines is essential for the enhanced motility for these osteosarcoma cells, suggesting the contribution of Src family kinase activity to the high metastatic potential of human osteosarcoma.

Results

General enhancement of tyrosine phosphorylation in high-metastatic HuO9 sublines

First, we confirmed the difference in motility between low- and high-metastatic sublines using Cell Culture Insert. High-metastatic sublines, M112 and M132, showed more than six times as high motility as low-metastatic sublines, L12 and L13 (data not shown). This result indicates that the motility of HuO9 sublines indeed correlates with their metastatic potential as previously reported (Nakano *et al.*, 2003).

To clarify the factors that determine the metastatic potential of HuO9 sublines, we compared expression patterns of phosphotyrosine-containing proteins between low- and high-metastatic sublines (Figure 1). General enhancement of tyrosine phosphorylation was observed in high-metastatic sublines, M112 and M132, as well as parental HuO9, which also has rather high metastatic potential (Nakano *et al.*, 2003). Among several phosphotyrosine-containing proteins showing elevated phosphorylation in high-metastatic sublines, the most striking difference was a broad band around 70 kDa (marked b in Figure 1). In addition, there were several other minor phosphotyrosine-containing proteins differentially expressed between low- and high-metastatic sublines, such as proteins around 60 kDa (marked c in Figure 1) and 120–130 kDa (marked a in Figure 1). These differences in tyrosine phosphorylation were consistent at different time points after plating (6 and 24 h) with and without fibronectin coating (Supplementary Figure 1 and data not shown).
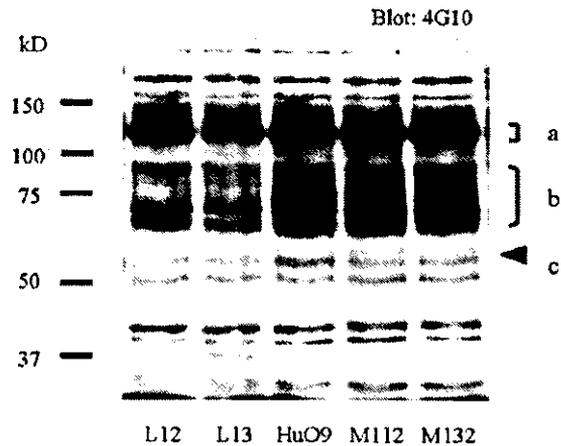

Figure 1 Elevated tyrosine phosphorylation of several proteins in high-metastatic sublines of HuO9 cells. Low-metastatic sublines (L12, L13), high-metastatic sublines (M112, M132) and parental HuO9 cells plated on plastic culture dishes for longer than 48 h were lysed for immunoblotting with anti-phosphotyrosine antibody 4G10. Hyperphosphorylated proteins in high-metastatic sublines are indicated on the right (a, b, c)

As candidate proteins of the difference around 120–130 kDa tyrosine phosphorylation, $p130^{Cas}$ and focal adhesion kinase (FAK) were examined using phospho-specific antibodies (Figure 2). $p130^{Cas}$ is a docking protein involved in the integrin signaling. We generated phospho-specific antibodies against several putative phosphorylation sites of $p130^{Cas}$ and used them for the analysis. As a result, elevated phosphorylation of Tyr 762 was found in high-metastatic sublines (2.5 times as much as low-metastatic sublines), while phosphorylation of Tyr 460 of $p130^{Cas}$ did not show obvious correlation with metastatic potential (Figure 2a). Tyr 460 represents tandem YDXP motifs in the substrate domain of $p130^{Cas}$, which binds (Crk) (Sakai *et al.*, 1994) or Nck (Schlaepfer *et al.*, 1997), and Tyr 762 consists of YDYV motif, which serves as a Src-binding site when phosphorylated (Nakamoto *et al.*, 1996). Expression of $p130^{Cas}$ did not vary significantly among each subline (Figure 2a).

FAK is a nonreceptor tyrosine kinase, which is also involved in the integrin signaling, and its Tyr 397 is autophosphorylated when FAK is activated (Schaller *et al.*, 1994). The expression of FAK and phosphorylation on Tyr 397 of FAK were analysed. However, no remarkable elevation of tyrosine-phosphorylated FAK was detected in high-metastatic sublines (Figure 2b).

To identify the phosphotyrosine-containing protein around 60 kDa, the expression level and tyrosine phosphorylation of Src family kinases was examined. Among the members of Src family kinases, only Fyn kinase had the tendency of hyperphosphorylation in high-metastatic sublines (Figure 2c). Tyrosine phosphorylation of c-Src, Yes, and Fgr, other members of Src family kinases that were examined, did not correlate
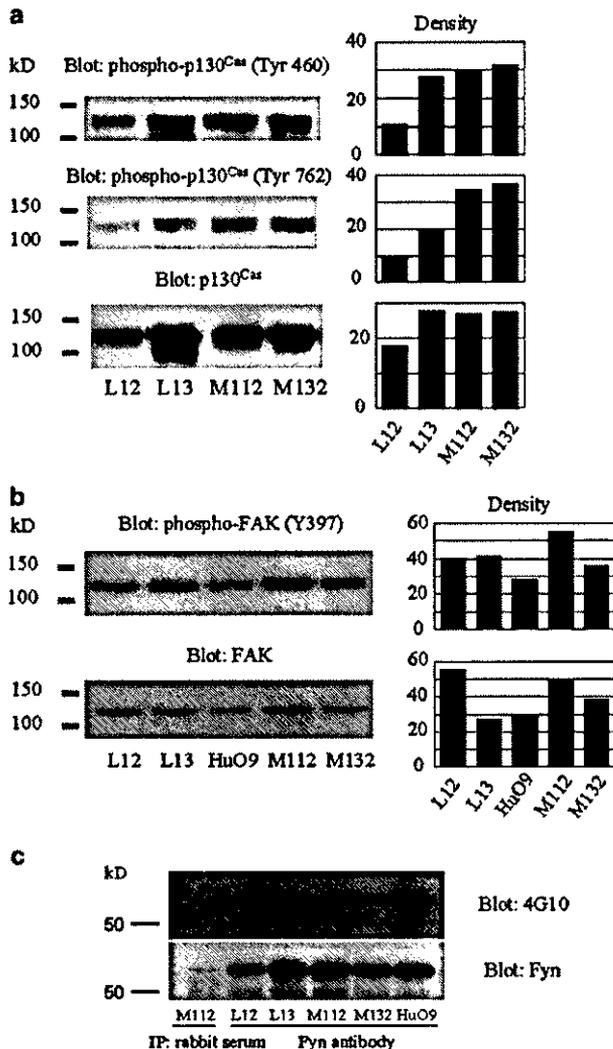
Figure 2 Elevated tyrosine phosphorylation of p130^Cas (Tyr 762) in high-metastatic sublines. (a) Whole-cell lysates from low-metastatic (L12, L13) and high-metastatic sublines (M112, M132) were immunoblotted for two kinds of anti-phospho-p130^Cas antibody (Tyr 460 representing the tandem YDXP motif, and Tyr 762 representing the YDYV motif in Src-binding domain) and p130^Cas antibody. Density of each blot was measured as described in Materials and methods. (b) Whole-cell lysates from low-metastatic (L12, L13), high-metastatic (M112, M132) and parental HuO9 were immunoblotted for anti-phospho-FAK antibody (Tyr 397) and anti-FAK antibody. Density of each blot was measured as described in Materials and methods. (c) Fyn kinase of low- and high-metastatic sublines was immunoprecipitated by anti-Fyn polyclonal antibody and subsequently immunoblotted with anti-phosphotyrosine antibody 4G10 or anti-Fyn antibody

with the metastatic potential (data not shown). However, absorption of Fyn by anti-Fyn antibody from lysates of low- and high-metastatic sublines could not remove the difference in tyrosine phosphorylation around 60 kDa (data not shown), indicating that not only Fyn contributes to the elevation of tyrosine phosphorylation around 60 kDa.

Overexpression and hyperphosphorylation of paxillin in high-metastatic HuO9 sublines

From the molecular size and the broad appearance of the 70 kDa protein, we estimated that this highly phosphorylated protein in high-metastatic sublines was paxillin. Using a specific antibody of phospho-paxillin (Tyr 118) for the blotting of whole-cell lysates, it was confirmed that high-metastatic sublines indeed contained a higher amount of tyrosine-phosphorylated paxillin in high-metastatic sublines (Figure 3A). It was also found that total paxillin expression was elevated in high-metastatic sublines (Figure 3A). As for both total paxillin and phospho-paxillin, high-metastatic sublines were estimated to contain about three to five times as much as low-metastatic sublines using densitometric analysis.

Absorption of paxillin by anti-paxillin antibody from lysates of low- and high-metastatic sublines remove most of the difference in tyrosine phosphorylation around 70 kDa (Figure 3B), indicating that paxillin mainly contributes to the elevation of tyrosine phosphorylation around 70 kDa.

Immunostaining of paxillin revealed that total paxillin and phospho-paxillin (Tyr 118) localize at focal adhesions, which were characterized at both ends of the actin filaments in L12 and M132 cells (Figure 3C). There was no significant change in the localization of paxillin by the metastatic potential of sublines, although the staining of total paxillin and phospho-paxillin were stronger in high-metastatic sublines than those in low-metastatic sublines (Figure 3D).

Src family kinase activity is elevated in the high-metastatic sublines

The general enhancement of tyrosine phosphorylation in high-metastatic sublines (Figure 1) suggests that the activity of some tyrosine kinases were enhanced in high-metastatic sublines. Therefore, we examined which tyrosine kinase is responsible for the high metastatic potential.

First, the difference in Src family kinase activity was investigated using Src-2 antibody, which is known to recognize wide ranges of Src family kinases. As a result, the activity of Src family kinases was elevated in the high-metastatic sublines (Figure 4a). The candidate for the Src family kinase responsible for the elevated kinase activity in high-metastatic sublines might be Fyn, which showed enhanced autophosphorylation in high-metastatic sublines (Figure 2c). We also examined the kinase activity of FAK and c-Abl, which are also reported to phosphorylate the tyrosine residues of paxillin. However, we observed a lack of correlation between kinase activity of FAK or c-Abl and metastatic potential (Figure 4b).

To check the influence of Src family kinase activity on cell motility elevated in high-metastatic sublines, cell migration assay was performed. In the high-metastatic sublines treated with PP2, an inhibitor of Src family kinases, motility was significantly suppressed, while in
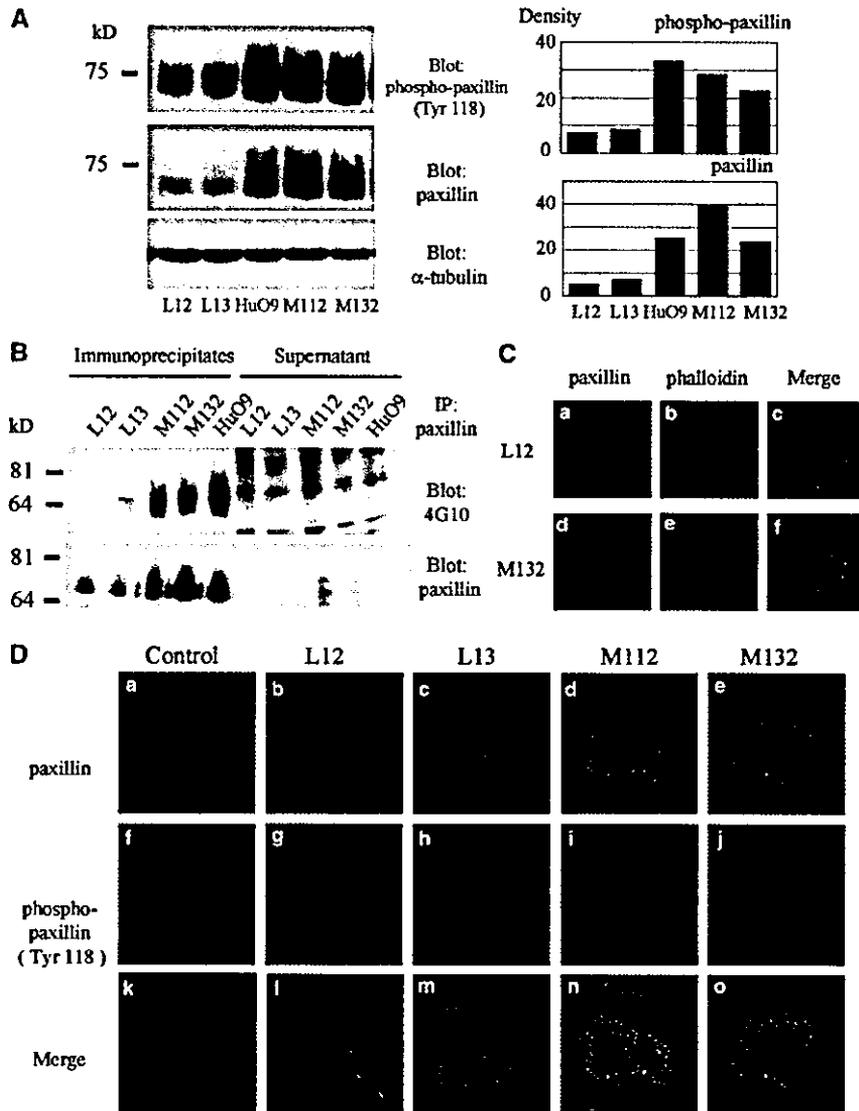
Figure 3 Overexpression and hyperphosphorylation of paxillin in high-metastatic sublines. (A) Whole-cell lysates from low-metastatic (L12, L13), high-metastatic (M112, M132) and parental HuO9 were immunoblotted for anti-phospho-paxillin antibody (Tyr 118), paxillin antibody and anti-α-tubulin antibody as an internal control. Densities of paxillin and phospho-paxillin blots are shown on the right. (B) Whole-cell lysates of low- and high-metastatic sublines and parental HuO9 cells were immunoprecipitated by monoclonal anti-paxillin antibody. Both immunoprecipitates and supernatants (indicated at the top) were subjected to immunoblotting analysis by anti-phosphotyrosine antibody 4G10 and anti-paxillin antibody. (C) L12 and M132 sublines were immunostained with anti-paxillin antibody (a, d: green), and chemically stained with phalloidin (b, e: red) at the same time. (D) Low- and high-metastatic sublines were immunostained with the antibody against paxillin (b–e: green) or phospho-paxillin (g–j: red). Superimposed confocal images (l–o: merge) demonstrate the portion of phosphorylated paxillin over the total paxillin. Images without first antibodies (a and f) are shown as negative controls. For comparison, panels were captured with identical gain and iris value and processed in the same way

the cells treated with PP3, inactive structural analog of PP2, their motility was not affected (Figure 4c). The effect of Src family kinase on the tyrosine phosphorylation of paxillin was also evaluated. When, high-metastatic sublines were treated with PP2, the tyrosine phosphorylation of paxillin was almost completely abolished, while the phosphorylation remained unchanged when the cells were treated with PP3 (Figure 4d). These results indicate that, in high-

metastatic sublines of HuO9, tyrosine phosphorylation of paxillin and enhanced cell motility are mostly dependent on the activity of Src family kinases.

Cell migration was attenuated by knocking down of paxillin expression in high-metastatic sublines

To evaluate the direct involvement of paxillin in the cell motility of the osteosarcoma cells, paxillin expression
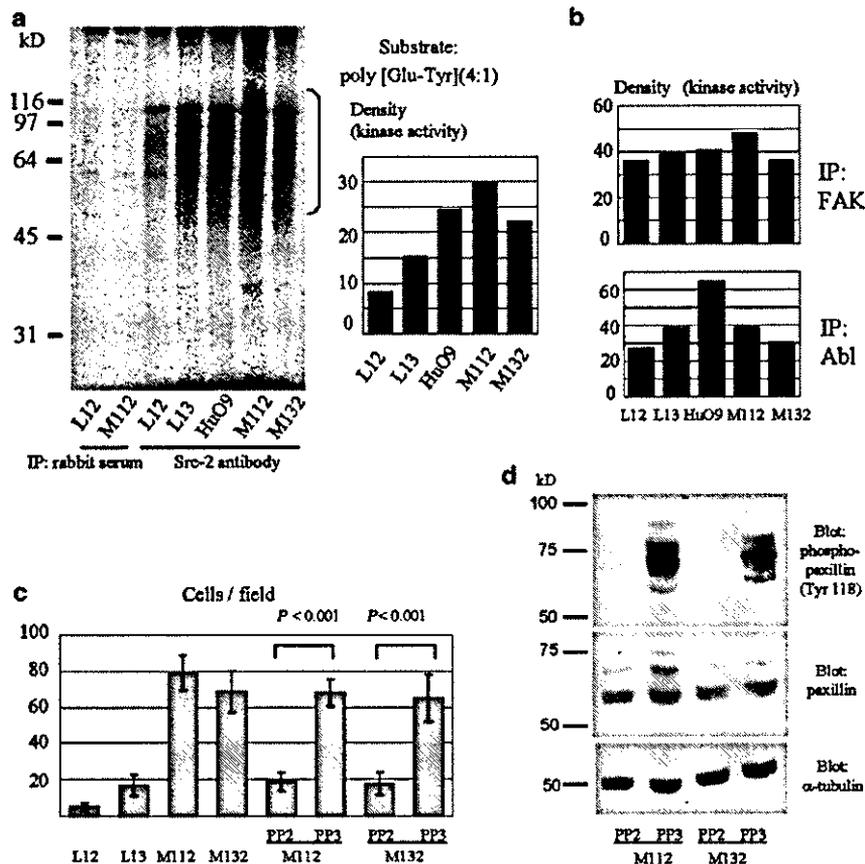
Figure 4 Elevated Src family kinase activity in high-metastatic sublines. (a) Elevated Src family kinase activity in high-metastatic sublines. Src family kinases of low- and high-metastatic sublines and parental HuO9 cell lysates were immunoprecipitated by Src-2 antibody. Lysates of L12 and M112 immunoprecipitated with preimmune rabbit serum were used as negative controls. Kinase activity was evaluated by phosphorylation of exogenous synthetic polypeptide poly[Glu-Tyr](4:1). The density of each smear (between 50 and 150 kDa, area shown by a bracket) was quantified. (b) FAK or c-Abl of low- and high-metastatic sublines and parental HuO9 were immunoprecipitated by monoclonal antibodies. To evaluate kinase activity, exogenous synthetic polypeptide poly[Glu-Tyr](4:1) was used. The kinase activities were quantified according to the same method as described in (a). (c) Src family kinase inhibitor PP2 (4-amino-5-(4-chlorophenyl)-7-(t-butyl)pyrazolo[3,4-d]pyrimidine) impairs the motility of high-metastatic sublines. Motility of low- and high-metastatic sublines and parental HuO9 cells was evaluated by migration assay as described in Materials and methods. As for high-metastatic sublines, M112 and M132, motility in the presence of 10 μM of PP2 or 10 μM of PP3 (4-amino-7-phenylpyrazol [3,4-d]pyrimidine) was also evaluated. The cells at the lower side of the filters were stained by Giemsa's stain solution and visualized under microscope at a magnification of × 200. Each bar represents the mean number of cells ± s.d. counted in five fields. (d) Src family kinase inhibitor PP2 abolishes tyrosine phosphorylation of paxillin. High-metastatic subline M112 and M132 were treated with 10 μM of PP2 or PP3 for 30 min prior to cell lysis. Whole-cell lysates were immunoblotted for anti-phospho-paxillin antibody, anti-paxillin antibody and anti-α-tubulin antibody

was knocked down using RNA interference (RNAi) in high-metastatic HuO9 sublines. Using a novel approach called the Dicer method to introduce a series of short interfering RNA (siRNA) into the cells, paxillin expression was suppressed by about 60%, while phospho-paxillin decreased by about 30% compared with LacZ siRNA-treated cells (Figure 5a).

Although the expression of paxillin was not completely suppressed, cell motility was impaired by about two-thirds by treatment with paxillin siRNA when compared with LacZ siRNA-treated cells (Figure 5b). This difference is statistically significant over nonspecific effects of siRNA on cell survival and motility.

This attenuation of motility was not observed when the expression of p130^{Cas} was knocked down using the Dicer method in high-metastatic sublines (Supplementary Figure 2a, b). These results indicate paxillin rather than p130^{Cas} is more closely associated with the motility of osteosarcoma sublines.

Overexpression of paxillin and elevation of Src family kinase activity synergistically enhance the motility of human osteosarcoma

To further examine the role of paxillin and its tyrosine phosphorylation on the motility of osteosarcoma sublines, the effect of transient transfection of GFP-paxillin

6

and its phenylalanine mutant of two tyrosines (2F mutant) was evaluated. In 2F mutant, two critical tyrosine phosphorylation sites at Tyr 31 and Tyr 118
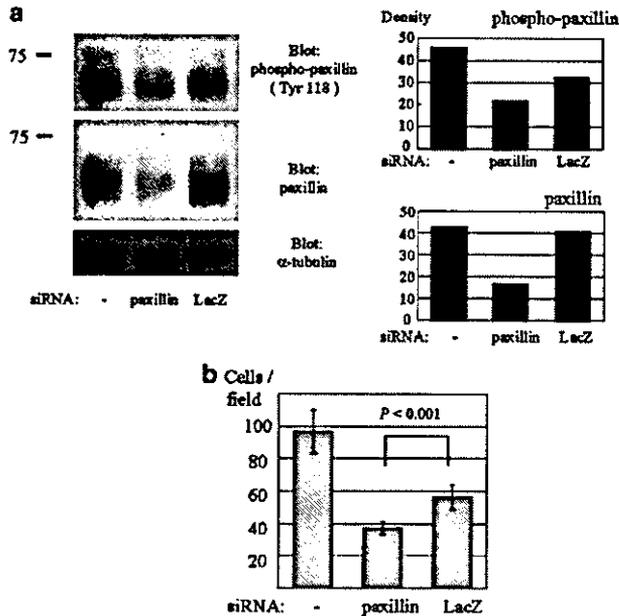
were mutated to phenylalanine, and these tyrosine residues were confirmed to be major phosphorylation sites by transient transfection of GFP-paxillin and GFP-2F mutant to COS-7 cells (Figure 6A).

Next, GFP-paxillin and GFP-2F mutant were transiently expressed in the low-metastatic subline, L12 (Figure 6B, arrowhead in lower panel). The tyrosine phosphorylation of GFP-paxillin was detected by phospho-paxillin (Tyr 118) antibody in L12 (Figure 6B, arrowhead in upper panel), although this polyclonal antibody showed slight reactivity even to the
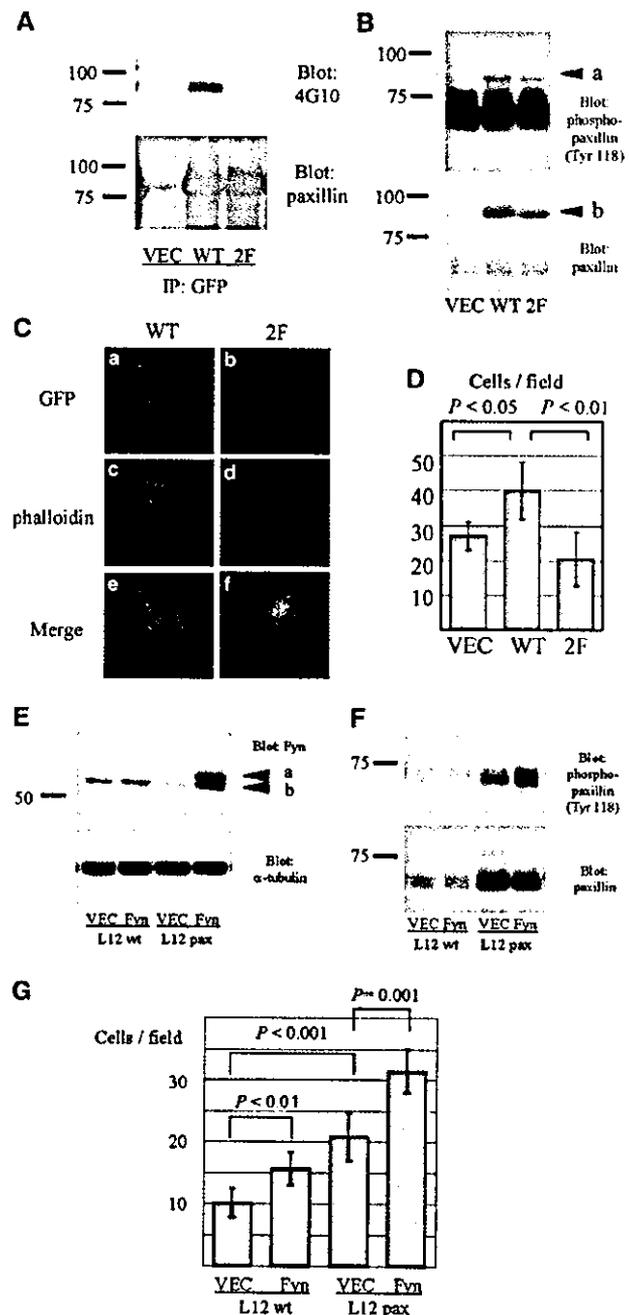

Figure 5 Cell migration was attenuated by knocking down of paxillin expression in high-metastatic sublines. (a) M112 subline was transfected with siRNA of paxillin or LacZ, or treated only with lipofection reagent ((−), as indicated at the bottom). Cells were lysed at 72 h from the transfection and whole-cell lysates were immunoblotted with the antibodies indicated. The density of each band is shown on the right. (b) M112 subline was transfected with siRNA or treated only with lipofection reagent as described above. Transfected cells were subjected to migration assay as described in Materials and methods

Figure 6 Overexpression of paxillin and elevation of Src family kinase activity synergistically enhance the motility of human osteosarcoma. (A) Cos-7 cells were transiently transfected with empty vector (VEC), GFP-paxillin (WT) or GFP-2F (Y31F, Y118F) mutant (2F). Cells were lysed at 48 h from the transfection and immunoprecipitated with anti-GFP antibody. Immunoprecipitates were subjected to immunoblotting analysis by anti-phosphotyrosine antibody 4G10 and anti-paxillin antibody. (B) L12 cells were transiently transfected with empty vector (VEC), GFP-paxillin (WT) or GFP-2F mutant (2F). Whole-cell lysates were immunoblotted for anti-phospho-paxillin antibody (Tyr 118) and paxillin antibody. GFP-paxillin and GFP-2F mutant were indicated (arrowhead a and b). (C) L12 cells transfected with GFP-paxillin or GFP-2F mutant were chemically stained with phalloidin. GFP (a, b: green) and phalloidin (c, d: red) were visualized with confocal microscopy. (D) L12 cells transfected with empty vector, GFP-paxillin or GFP-2F mutant were subjected to migration assay as described in Materials and methods. (E, F) L12 cells (L12 wt) or paxillin-FLAG-expressing stable cells (L12 pax) were transiently transfected with empty vector (VEC) or Fyn-FLAG (Fyn). Whole-cell lysates were immunoblotted for the antibodies indicated. Fyn-FLAG (arrowhead a) and endogenous Fyn (arrowhead b) were shown in (E) upper panel. (G) L12 cells or paxillin-FLAG-expressing stable cells that were transiently transfected with empty vector or Fyn-FLAG were subjected to migration assay as described in Materials and methods

2F mutant of paxillin. Both GFP-paxillin and GFP-2F mutant were confirmed to localize at focal adhesions (Figure 6C).

Cell motility was enhanced by the transient expression of GFP-paxillin compared with the transfection of GFP-2F mutant or empty vector (Figure 6D). This indicates that the amount of wild-type paxillin is positively correlated with the motility of osteosarcoma sublines. Considering that GFP-2F mutant could localize at focal adhesions (Figure 6C), the lack of motility-promoting effect of GFP-2F mutant was due to the absence of phosphorylation at Tyr 31 and Tyr 118.

The synergistic effect of paxillin overexpression and Src family kinase activity was examined using a low-metastatic subline, L12. We established L12 cells that stably express more than five times as much an amount of exogenous paxillin as the wild-type L12 subline, which is a similar level of endogenous paxillin in the high-metastatic sublines. FLAG epitope-tagged Fyn was transiently transfected to wild-type L12 cells and paxillin-overexpressing L12 cells (Figure 6E). Enhancement of tyrosine phosphorylation of paxillin was observed in Fyn-FLAG-transfected cells compared with mock-transfected cells in both wild-type L12 and paxillin-overexpressing L12 cells (Figure 6F). Cell migration assay reveals that overexpression of both Fyn-FLAG and paxillin-FLAG significantly enhances the cell motility of L12 cells (Figure 6G). This result of cell migration was correlated with the amount of phospho-paxillin in the cells (Figure 6F, upper panel), which suggests that overexpression of paxillin and Fyn contributes to the enhanced motility through the tyrosine phosphorylation of paxillin.

Discussion

We have shown the general enhancement of tyrosine phosphorylation in high-metastatic HuO9 sublines, and the elevated activation of Src family kinase. Among the substrates of Src family kinase, prominent phosphorylation of paxillin along with elevated expression of paxillin was observed in the high-metastatic sublines.

Since human osteosarcoma cell lines suitable for metastatic study were not available, results of previous biochemical analysis on metastatic osteosarcoma were derived from murine models (Khanna et al., 2001, 2004; Iwaya et al., 2003). The present study is the first biochemical analysis on human metastatic osteosarcoma. We used four independent, but genetically close sublines of osteosarcoma that are excellent tools for analysis of signal alteration in the process of acquiring metastatic potential. The high-metastatic sublines were established by in vivo selection and the low-metastatic sublines by the dilution plating method. Considering that malignant tumors contain subpopulations of different metastatic capabilities, these selection methods resemble authentic events during the progression of osteosarcoma. Moreover, these sublines were estab-

lished without any manipulation of genes, which minimizes the artificial effects on our study.

In these sublines of human osteosarcoma, the results of cell motility assay clearly reflected metastatic potential (Nakano et al., 2003). This is reasonable because the properties of cancer cells measured by cell migration assay such as cell movement and ability to interact with extracellular matrix are critical factors during tumor metastasis. Therefore in this study, cell motility was used as an indicator of metastatic potential.

Elevation of Src family kinase activity in metastases was reported in human colorectal cancer (Talamonti et al., 1993) and in human melanoma (Marchetti et al., 1998). According to these reports, there is clear difference in the activated member of Src family kinase among types of tumors. Talamonti et al. showed increased activity of c-Src in liver metastases compared to primary tumor. Marchetti et al. used brain metastatic sublines and found that kinase activity of Yes, not c-Src, was elevated compared to low-metastatic cells. We recently reported that, in a metastatic model of murine melanoma cell lines, kinase activity of Fyn was elevated in high-metastatic sublines, and interacted with cortactin (Huang et al., 2003). Although not as significant as in the case of murine melanoma, Fyn will also be a candidate for the responsible kinase for metastatic potential of human osteosarcoma. Other members of Src family kinase with relatively low expression, such as c-Src, or with relatively low kinase activity do not appear to be involved in regulation of metastatic potential.

In osteosarcoma, elevated phosphorylation of YDYV motif in p130^{Cas} in high-metastatic sublines (Figure 2a) is a possible clue to Src family activation because phosphorylated YDYV motif in p130^{Cas} stabilizes the active form of Src family kinases by binding with the SH2 domain of Src family kinases (Nakamoto et al., 1996; Burnham et al., 2000). This type of molecule may function as a regulator of Src family kinases that causes activation of Src family kinases in osteosarcoma cells, although the contribution of phosphorylated p130^{Cas} may be low considering the small effect of RNAi on the cell motility.

Although this is the first report on hyperphosphorylation of paxillin in a metastatic tumor, some studies investigated the relationship of cell motility and tyrosine phosphorylation of paxillin. Tyr 31 and Tyr 118 of paxillin are phosphorylated upon cell adhesion (Burridge et al., 1992) and Src family tyrosine kinases (Klinghoffer et al., 1999), FAK (Schaller and Parsons, 1995), and c-Abl (Lewis and Schwartz, 1998) are reported to phosphorylate these sites. The roles of phospho-paxillin on cell motility are still controversial. Migration-promoting effect of phospho-paxillin was demonstrated by using Nara bladder tumor II (NBTII) cells (Petit et al., 2000), while migration-inhibitory effect was shown by using NMuMG cells, MM-1 cells and Cos 7 cells (Yano et al., 2000; Tsubouchi et al., 2002). Our results have added another example of the migration-promoting effects of phospho-paxillin.

The migration-promoting effect of phospho-paxillin might be due to interaction with Crk (Schaller and Parsons, 1995). Crk interacts with a cellular protein DOCK180, which binds directly and activates small GTPase Rac1 (Kiyokawa et al., 1998). Activation of this pathway provides a link between paxillin–Crk association and cell motility.

The binding partners of phospho-paxillin seem to vary among tumor types and may provide some clue for the controversy between migration-promoting and -inhibitory effect of phospho-paxillin. In NMuMG cells, in which phosho-paxillin exerts migration inhibitory effect, phospho-paxillin was shown to bind p120Ras-GAP and RhoA activity was suppressed as a downstream of signal transduction (Tsubouchi et al., 2002). Therefore, it is also possible that SH2 domain-containing molecule other than Crk may function as a binding partner of phospho-paxillin and send a positive signal for cell motility in osteosarcoma cells.

We observed the impaired motility by knocking down the expression of paxillin and showed the direct effect of paxillin on cell migration. Paxillin-knocked-down cells showed 67% migration activity compared to LacZ siRNA-treated cells. One reason for this rather weak motility suppression is the partial effect of RNAi, as 40% of paxillin and 68% of phospho-paxillin remained after the treatment with paxillin siRNA compared to LacZ siRNA-treated cells. Another possible reason is the existence of other factors that enhance the metastatic potential independently of paxillin. However, considering the partial effect of RNAi, it can be estimated that paxillin has a significant contribution to high-metastatic phonotype.

We examined the contribution of p130^{Cas}, which is another substrate of Src family kinase and involved in the integrin signaling. As a result, suppression of p130^{Cas} expression did not affect the motility of high-metastatic osteosarcoma cells, which supports the relative importance of paxillin in the motility of osteosarcoma cells.

FAK is also known as a binding partner and a substrate of Src family kinase. However, in the osteosarcoma sublines, the tyrosine phosphorylation of FAK was not correlated with the activity of Src family kinase. This may suggest that, in the case of human osteosarcoma, the phosphorylation of FAK reflects other kinase activity including autophosphorylation and is not strongly associated with metastatic potentials.

We have shown the migration-promoting effect of phosho-paxillin by overexpression of GFP-paxillin and its mutant. Expression of exogenous GFP-paxillin enhanced the cell motility in the low-metastatic subline, while expression of GFP-2F mutants did not. Furthermore, we showed paxillin overexpression and Src family activity could contribute to the high metastatic potential of osteosarcoma. Expression of Fyn-FLAG and paxillin-FLAG at the same time in the L12 subline promoted the motility synergistically, although it did not enhance the motility to the extent of high-metastatic sublines, probably because of the existence of other factors which contribute to the high-metastatic potential of osteosarcoma. These results strongly suggest that this cooperative function of Src family kinase and paxillin also works in endogenously expressed proteins and play a major role in high-metastatic phenotype of osteosarcoma cells.

Then, what is the mechanism of overexpression of paxillin in high-metastatic sublines of human osteosarcoma? The locus of paxillin, 17p8q, is not included in the areas where comparative genomic hybridization (CGH) analysis revealed that gene amplification is frequent in human osteosarcoma (Batanian et al., 2002; Squire et al., 2003; Lau et al., 2004). Paxillin mRNA in high-metastatic sublines is at most 1.7 times compared to that in low-metastatic sublines by cDNA microarray analysis (Nakano et al., personal communication). Considering high-metastatic sublines express about five times as much paxillin as low-metastatic sublines, paxillin may be highly stable and degraded slowly in high-metastatic sublines.

In conclusion, this study provides information on the importance of phospho-paxillin during metastasis of human osteosarcoma. We have shown that enhancement of Src family kinase activity and overexpression of paxillin synergistically contribute to the high metastatic potential of human osteosarcoma through hyperphosphorylation of paxillin. Further biochemical analysis is needed to clarify the phosphotyrosine-dependent binding partner with paxillin, since the downstream pathway specific to tumor metastasis is a potential therapeutic target. If Src family kinases are activated by a specific mechanism in metastatic osteosarcoma, that would also be an attractive therapeutic target. These themes deserve investigation to improve the extremely poor prognosis of metastatic osteosarcoma.

Materials and methods

Antibodies and reagents

Anti-phosphotyrosine antibody 4G10 was purchased from Upstate Biotechnology. Phospho-specific antibodies against Tyr 460 and Tyr 762 of p130^{Cas} were raised by immunizing rabbits with peptide CAEDVYDVP and CMEDYDYVHL, respectively, and affinity purified. As anti-p130^{Cas} antibody, polyclonal Cas2 antibody was used as described previously (Sakai et al., 1994). Monoclonal antibody against FAK was from BD Transduction Laboratories. Polyclonal antibody against phospho-FAK (Tyr 397) was purchased from Upstate Biotechnology. Monoclonal antibody against c-Src (GD11) was from Upstate Biotechnology. Polyclonal antibodies against Fyn (Fyn-3), Fgr (N-47) and pan-Src (Src-2) were from Santa Cruz Biotechnology. Monoclonal antibodies against Yes, Hck, Lck and Lyn were purchased from BD Transduction Laboratories. Monoclonal antibody against paxillin was from Zymed Laboratories Inc. Polyclonal antibody against phospho-paxillin (Tyr 118) was purchased from Cell Signaling. Anti-α-tubulin antibody (B-5-1-2) was purchased from SIGMA. Monoclonal antibody against Abl was from BD Biosciences. Polyclonal antibody against GFP (598B) was from Medical and Biological Laboratories. HRP-conjugated anti-mouse antibody was purchased from Amersham Pharmacia. Alexa Fluor 488 goat anti-mouse IgG, Alexa Fluor 594 goat anti-rabbit IgG and Alexa Fluor 546 phalloidin were

purchased from Molecular Probe. Normal rabbit serum was from DakoCytomation. Src family kinase inhibitor PP2 and the structural analog PP3 were purchased from Calbiochem-Novabiochem Ltd.

Plasmids

A FLAG epitope-tagged paxillin construct was generated by amplifying the coding sequence of human paxillin by PCR using the primers 5'-CGTACCTCGAGGCCATGGAC-GACCTCGACGC-3' and 5'-GGAATT-CATTTGTCGTCGTCGTCCTTGTAGTCGCAGAA-GAGCTTGAGGAAGC-3'. This resulted in a fragment with an *XhoI* site (underlined), a sequence encoding the FLAG epitope (DYKDDDDK), followed by a termination codon and an *EcoRI* site (underlined). This fragment was then digested with *XhoI* and *EcoRI* sequentially, and ligated into the mammalian expression vector pcDNA3.1(−)/Myc-His B (Invitrogen).

GFP-paxillin is a kind gift from Dr Y Sawada (Department of Biological Sciences, Columbia University). Phenylalanine mutant at Tyr 31 and Tyr 118 was generated by amplifying GFP-paxillin with following primers. 5'-CGGCCTGTGTTCTTAAGCGAGGAGACCCCCTTCT-CATACCCAAC-3' and 5'-GTTGGGTATGA-GAAGGGGGTCTCCTCGCTTAAGAACACAGGCCG-3' were used for Tyr 31, and 5'-CCGTGCTCTAGAGTGGGA-GAGGAGGAGCACGTGTTCAGCTTCCC-3' and 5'-GGGAAGCTGAACACTGTCTCCTCCTCTCCCACTC-TAGAGCACGG-3' were used for Tyr 118.

A FLAG epitope-tagged Fyn construct was generated by amplifying the RT–PCR product of human colon cancer cell line, HCT116, by PCR using the primers 5'-GGATC-CATGGGCTGTGTGCAATGTAAG-3' and 5'-GTTAACT-CACTTGTCGTCATCGTCCTTGTAGTCCAGGTTTT-CACCAGGTTG-3'. This PCR product was first inserted into pGEM-T Easy vector (Promega), followed by excision with *EcoRI*, and ligated into the mammalian expression vector pcDNA3.1(−)/Myc-His A (Invitrogen).

Cell culture and transfection

A human osteosarcoma cell line, HuO9, and its high-metastatic (M112, M132) and low-metastatic (L12, L13) sublines have been described previously (Nakano *et al.*, 2003). Osteosarcoma cells were maintained in RPMI 1640 medium with 10% fetal bovine serum (FBS) at 37°C with 5% CO_2. Cos-7 cells were maintained in Dulbecco's modified Eagle's medium (DMEM) with 10% FBS at 37°C with 5% CO_2. Transfection was performed by using FuGENE 6 (Roche) according to the manufacturer's instruction. Selection of clones was performed by using geneticin (Sigma) at the concentration of 30 μg/ml.

Immunoblotting and immunoprecipitation

Before extracting cell lysates, osteosarcoma cells were cultured for at least 48 h to ensure complete cell adhesion to culture dishes unless otherwise indicated. Cells were lysed in 1% Triton X-100 buffer (50 mM HEPES, 150 mM NaCl, 10% glycerol, 1% Triton-X 100, 1.5 mM $MgCl_2$, 1 mM EGTA, 100 mM NaF, 1 mM Na_3VO_4, 10 μg/ml aprotinin, 10 μg/ml leupeptin, 1 mM phenylmethylsulfonyl fluoride), and insoluble materials were removed by centrifugation. To investigate the effect of PP2 treatment, cells were treated with 10 μM of PP2 or 10 μM of PP3 for 30 min prior to harvesting cells.

Protein concentration was measured by BCA Protein Assay (PIERCE) and the protein aliquots were separated by SDS–

PAGE. Gels were transferred to a polyvinylidene difluoride membrane (Millipore) and subjected to immunoblotting. After blocking in 5% skim milk/TBST (100 mM Tris-HCl pH 8.0, 150 mM NaCl, 0.05% Tween 20) for 1 h, blots were incubated with appropriate primary antibodies. In case of 4G10 stain, blocking was performed with 5% bovine serum albumin (BSA) which was used instead of skim milk. Blots were then washed three times with TBST, incubated with HRP-conjugated secondary antibodies for 30 min, washed twice by TBST and twice with TBS (100 mM Tris-HCl pH 8.0, 150 mM NaCl), and visualized by autoradiography using chemiluminescence reagent (Western Lighting, Perkin Elmer).

The images were captured by molecular imager GS800 (BIO-RAD) and the density of each smear was quantified by Quantity One (BIO-RAD).

For immunoprecipitation, aliquots of protein were mixed with appropriate antibodies and incubated for 1 h on ice. Then, samples were rotated with protein A- or protein G-sepharose beads (Amersham Pharmacia) for 2–12 h at 4°C. After the beads were washed four times with 1% Triton-X 100 buffer, the samples were boiled in sample buffer (0.1 M Tris-HCl pH 6.8, 2% SDS, 0.1 M dithiothreitol, 10% glycerol, 0.01% bromophenol blue) for 5 min and analysed by SDS–PAGE.

Immunocytochemistry

Cells were grown on 12-mm circle cover glasses (Fisher) in 24-well plates, washed three times with phosphate-buffered saline (PBS), fixed with 4% paraformaldehyde/0.1 M phosphate buffer for 5 min at room temperature, washed once with PBS, and permeabilized with 0.2% Triton-X 100 in PBS for 10 min. After another washing step with PBS and blocking in 5% goat serum and 3% BSA/TBST for 30 min, cells were incubated with anti-paxillin antibody (1:2000) and anti-phospho-paxillin antibody (1:250) in 5% goat serum and 3% BSA/TBST for 1 h at room temperature. Cells were washed three times with PBS and incubated with appropriate second antibodies (Molecular Probe) (1:2000) in 5% goat serum and 3% BSA/TBST. When actin was stained with phalloidin, Alexa Fluor phalloidin was combined with second antibody at the concentration of 1 U/ml.

After cells were washed three times with PBS, cover glasses were mounted in 1.25% DABCO, 50% PBS, 50% glycerol and visualized using a Radiance 2100 confocal microscopic system (BIO-RAD).

In vitro kinase assay

For kinase assay, fresh cell lysate was prepared and mixed with the antibody of interest for 1 h on ice. Then, samples were rotated with protein A-sepharose or protein G-sepharose for 1 h at 4°C. The beads were consequently washed with 1% Triton-X 100 buffer and kinase buffer (50 mM Tris HCl, pH 7.4, 50 mM NaCl, 10 mM $MgCl_2$, 10 mM $MnCl_2$) three times, respectively. Kinase reaction was performed in 30 μl of kinase buffer with 10 μg of synthetic polypeptides poly[Glu-Tyr](4:1) (Sigma) as exogenous substrate and 5 μCi of [γ-32P]ATP (ICN) at room temperature for 1 h. Kinase reaction was stopped by the addition of SDS–PAGE sample buffer (0.1 M Tris-HCl pH 6.8, 2% SDS, 0.1 M dithiothreitol, 10% glycerol, 0.01% bromophenol blue). The samples were boiled for 5 min and analysed by SDS–PAGE using 8% polyacrylamide gel. The gels were then dried and exposed to autoradiography. The images were captured by molecular imager GS800 (BIO-RAD) and the density of each smear (area shown by a bracket) was quantified by Quantity One (BIO-RAD).

Cell migration assay

Cell migration assay was performed by using Cell Culture Insert with $8.0\,\mu m$ pore size PET filter (Becton Dickinson). Prior to the assay, the lower surface of the filter was immersed for 30 min in $10\,\mu g/ml$ fibronectin (Sigma) diluted with PBS. Next, $700\,\mu l$ of RPMI 1640 medium with 10% FCS was added to the lower chamber. Then, 5×10^4 cells were suspended in $300\,\mu l$ of RPMI 1640 medium with 10% FCS and added to the upper chamber.

After incubation for 24 h at 37°C in a humid 5% CO_2 atmosphere, the cells on the upper surface of the filter were completely removed by wiping with cotton swabs. The cells on the lower surface of the filter were fixed in methanol for 30 min, washed with PBS, and then stained with Giemsa's stain solution (Muto Pure Chemicals Co. Ltd.) for 30 s. After washing three times with PBS, the filters were mounted on a glass slide. The cells on the lower surface were counted from photographs taken of at least five fields at a magnification of $\times 200$ under the microscope. Student's t-test was used to analyse data from these experiments. To investigate the effect of PP2 treatment, cells were allowed to migrate in the presence of $10\,\mu M$ of PP2 or $10\,\mu M$ of PP3.

RNAi analysis

siRNA of human paxillin and p130^{Cas} was generated using BLOCK-iT RNAi TOPO Transcription Kit and BLOCK-iT Complete Dicer RNAi Kit (Invitrogen) according to the manufacturer's instructions. In the generation of siRNA for paxillin, 936 bp from the initiation codon of human paxillin

were chosen as the target sequence, and amplified by PCR using the primers, 5'-ATGGACGACCTCGACGCC-3' and 5'-GTTCAGGTCAGACTGCAGGC-3'. As for p130^{Cas}, 866 bp was chosen as the target sequence, and amplified with the primers, 5'-ACACCATGAACCACCTGAACGTG-3' and 5'-ATACACCTCCAGCAACGGGT-3'.

siRNA of LacZ was generated in the same procedure as paxillin siRNA, and was used as a negative control. Transfection was performed with Lipofectamine 2000 (Invitrogen) and the effect was analysed 72 h after the transfection.

Abbreviations

BSA, bovine serum albumin; Cas, Crk-associated substrate; FAK, focal adhesion kinase; FBS, fetal bovine serum; PBS, phosphate-buffered saline; PP2, 4-amino-5-(4-chlorophenyl)-7-(t-butyl)pyrazolo[3,4-d]pyrimidine; PP3, 4-amino-7-phenyl-pyrazol [3,4-d]pyrimidine; RNAi, RNA interference; SH2, Src homology 2 domain; siRNA, short interfering RNA.

References

Batanian JR, Cavalli LR, Aldosari NM, Ma E, Sotelo-Avila C, Ramos MB, Rone JD, Thorpe CM and Haddad BR. (2002). *Mol. Pathol.*, **55**, 389–393.

Burnham MR, Bruce-Staskal PJ, Harte MT, Weidow CL, Ma A, Weed SA and Bouton AH. (2000). *Mol. Cell. Biol.*, **20**, 5865–5878.

Burridge K, Turner CE and Romer LH. (1992). *J. Cell. Biol.*, **119**, 893–903.

Huang J, Asawa T, Takato T and Sakai R. (2003). *J. Biol. Chem.*, **278**, 48367–48376.

Huth JF and Eilber FR. (1989). *Arch. Surg.*, **124**, 122–126.

Iwaya K, Ogawa H, Kuroda M, Izumi M, Ishida T and Mukai K. (2003). *Clin. Exp. Metast.*, **20**, 525–529.

Khanna C, Khan J, Nguyen P, Prehn J, Caylor J, Yeung C, Trepel J, Meltzer P and Helman L. (2001). *Cancer Res.*, **61**, 3750–3759.

Khanna C, Wan X, Bose S, Cassaday R, Olomu O, Mendoza A, Yeung C, Gorlick R, Hewitt SM and Helman LJ. (2004). *Nat. Med.*, **10**, 182–186.

Kimura K, Nakano T, Park YB, Tani M, Tsuda H, Beppu Y, Moriya H and Yokota J. (2002). *Clin. Exp. Metast.*, **19**, 477–485.

Kiyokawa E, Hashimoto Y, Kobayashi S, Sugimura H, Kurata T and Matsuda M. (1998). *Genes Dev.*, **12**, 3331–3336.

Klinghoffer RA, Sachsenmaier C, Cooper JA and Soriano P. (1999). *EMBO J.*, **18**, 2459–2471.

Lau CC, Harris CP, Lu XY, Perlaky L, Gogineni S, Chintagumpala M, Hicks J, Johnson ME, Davino NA, Huvos AG, Meyers PA, Healy JH, Gorlick R and Rao PH. (2004). *Genes Chromosomes Cancer*, **39**, 11–21.

Lewis JM and Schwartz MA. (1998). *J. Biol. Chem.*, **273**, 14225–14230.

Marchetti D, Parikh N, Sudol M and Gallick GE. (1998). *Oncogene*, **16**, 3253–3260.

Meyers PA, Heller G, Healey JH, Huvos A, Applewhite A, Sun M and LaQuaglia M. (1993). *J. Clin. Oncol.*, **11**, 449–453.

Nakamoto T, Sakai R, Ozawa K, Yazaki Y and Hirai H. (1996). *J. Biol. Chem.*, **271**, 8959–8965.

Nakano T, Tani M, Ishibashi Y, Kimura K, Park YB, Imaizumi N, Tsuda H, Aoyagi K, Sasaki H, Ohwada S and Yokota J. (2003). *Clin. Exp. Metast.*, **20**, 665–674.

Pawson T. (2004). *Cell*, **116**, 191–203.

Petit V, Boyer B, Lentz D, Turner CE, Thiery JP and Valles AM. (2000). *J. Cell. Biol.*, **148**, 957–970.

Sakai R, Iwamatsu A, Hirano N, Ogawa S, Tanaka T, Mano H, Yazaki Y and Hirai H. (1994). *EMBO J.*, **13**, 3748–3756.

Schaller MD. (2001). *Oncogene*, **20**, 6459–6472.

Schaller MD, Hildebrand JD, Shannon JD, Fox JW, Vines RR and Parsons JT. (1994). *Mol. Cell. Biol.*, **14**, 1680–1688.

Schaller MD and Parsons JT. (1995). *Mol. Cell. Biol.*, **15**, 2635–2645.

Schlaepfer DD, Broome MA and Hunter T. (1997). *Mol. Cell. Biol.*, **17**, 1702–1713.

Squire JA, Pei J, Marrano P, Beheshti B, Bayani J, Lim G, Moldovan L and Zielenska M. (2003). *Genes Chromosomes Cancer*, **38**, 215–225.

Talamonti MS, Roh MS, Curley SA and Gallick GE. (1993). *J. Clin. Invest.*, **91**, 53–60.

Tsubouchi A, Sakakura J, Yagi R, Mazaki Y, Schaefer E, Yano H and Sabe H. (2002). *J. Cell. Biol.*, **159**, 673–683.

Tsuchiya H, Kanazawa Y, Abdel-Wanis ME, Asada N, Abe S, Isu K, Sugita T and Tomita K. (2002). *J. Clin. Oncol.*, **20**, 3470–3477.

Turner CE. (2000). *Nat. Cell. Biol.*, **2**, E231–E236.